expression; expression of HCN2 and HCN4 is unaffected [13]. Moreover, none of the animal models of cardiac hypertrophy develop lethal arrhythmias. On the other hand, transgenic mice overexpressing a dominant-negative neuron-restricted silencing factor mutant (dnNRSF-Tg) die from ventricular tachyarrhythmia [9]. In the dnNRSF-Tg ventricle, robust increases in the expression of fetal cardiac channels, including HCN2 and HCN4 as well as CACNA1G and CACNA1H, two T-type Ca^{2+} channel subunits, have been reported [9], and blockade of HCN channels using ivabradine was recently shown to improve survival among dnNRSF-Tg mice [10]. This result is consistent with the potential arrhythmogenicity of HCN channels. It appears, however, that the overexpression of CACNA1G does not, by itself, provoke arrhythmias or SAPs in mouse ventricular myocytes; it only increases Ca^{2+} transients and induces mild cardiac hypertrophy [19]. Likewise, we showed that the overexpression of HCN2 is not, by itself, sufficient to induce lethal arrhythmia, but it induced an idioventricular rhythm under excessive β adrenergic stimulation. DADs are frequently observed in the myocytes isolated from hypertrophied heart. However, as shown in the present study, DADs were not induced by the overexpression of fetal type cardiac channels. These result suggested that the mechanism of ectopic automaticity in HCN2-Tg may be fundamentally different from that in hypertrophied heart.

In the present study, β-adrenergic stimulation consistently depolarized the RMP of HCN2-Tg myocytes. However, the magnitude of the depolarization did not directly correlate with the occurrence of SAPs, as depolarized RMPs in quiescent HCN2-Tg myocytes did not significantly differ from the MDPs of the SAPs. Why some cardiac myocytes (76%) exhibited SAPs while others (24%) did not remains unclear. In studies attempting to generate a "biological pacemaker" by overexpressing HCN2 in ventricular myocytes, the simultaneous overexpression of voltage-gated Na^+ channels (SkM1) was required for stable firing of SAPs [20]. This suggests, cell-to-cell variation in I_{Na} density may determine whether or not HCN2-Tg myocytes exhibit SAPs. In addition, I_{Na} and the T-type Ca^{2+} current ($I_{Ca\text{-}T}$) are activated at a similar range of membrane potentials [21]. Thus, the simultaneous overexpression of $I_{Ca\text{-}T}$ and I_h might induce stable SAPs in transgenic model mice and in hypertrophied hearts.

The firing rates of SAPs in HCN2-Tg myocytes were much less than 600 bpm. Because the heart rates of mice can easily increase to more than 700 bpm during β-adrenergic stimulation, the automaticity of HCN2-Tg ventricular myocytes may be masked by physiological pacing mediated via the cardiac conduction system [22,23]. Indeed, in this study ISO-induced ectopic ventricular rhythm in HCN2-Tg mice consistently preceded AV dissociation. Under physiological conditions, the pacemaker activity of the SA node might overdrive the idioventricular rhythm.

The repolarization phase of ventricular APs is primarily governed by activation of multiple K^+ currents, including I_{to}, the fast- and slow delayed rectifier K^+ currents (I_{Kr} and I_{Ks}; also known as HERG and KVLQT1), and I_{K1} [24–27]. This redundancy of repolarizing currents is called the "repolarization reserve" [28]. In the present study, we showed that when APs were recorded using the ruptured whole-cell patch method, the transgenic overexpression of HCN2 in mouse ventricular myocytes reduced the repolarization reserve and prolonged APD at the membrane potentials more negative than −35 mV. These results appear to be consistent with the observations reported in $HCN3^{-/-}$ myocytes, although the changes in APD were in the opposite direction in HCN2-Tg myocytes: in $HCN3^{-/-}$ myocytes, APD was shortened by

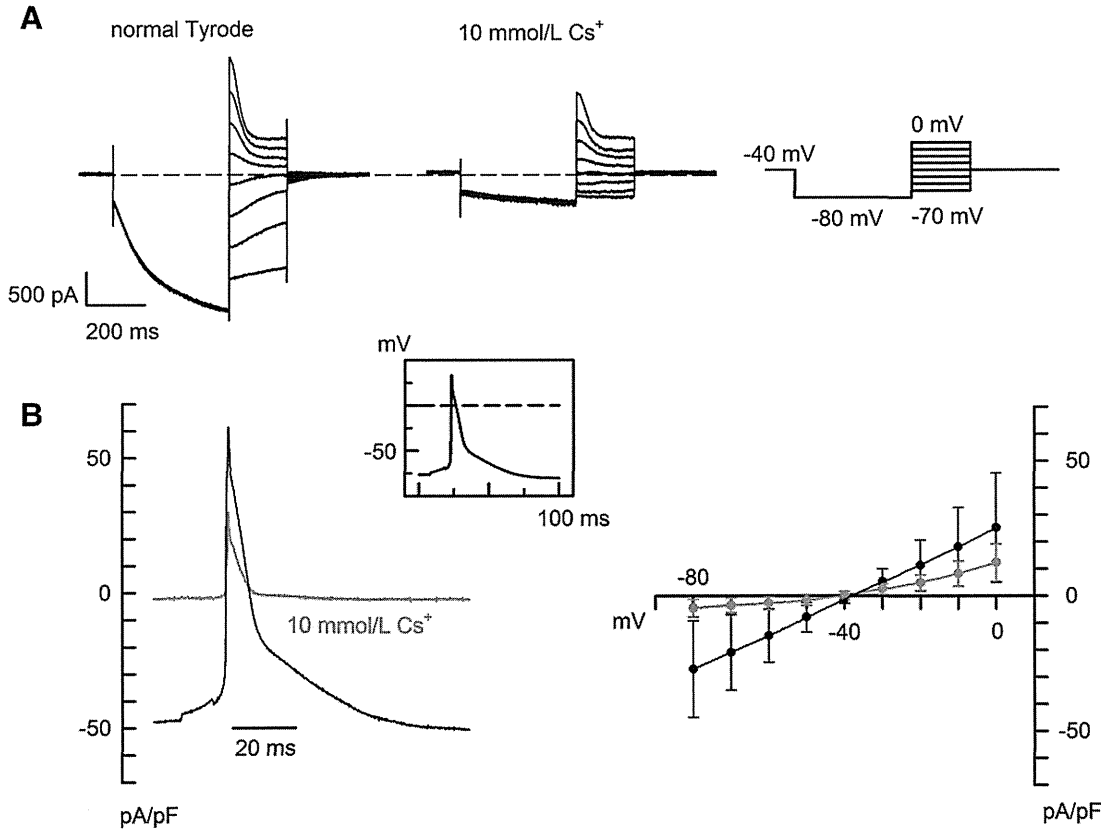

Fig. 7. Contribution of I_h tail currents to the repolarization phase of induced APs (A) HCN2 channels heterologously expressed in CHO cells were activated using a square pulse protocol (shown in the right panel). Family of I_h current before (left) and after (center) the application of 10 mmol/L Cs^+. The pipette solution contained 1 mmol/L cAMP. Note that the direction of the tail current reversed between −30 and −40 mV. (B) AP-shaped command pulses (inset) were applied to HCN2-expressing CHO cells at 0.5–5 Hz. The AP shape was sampled from HCN2-Tg myocytes in the presence of 0.3 μmol/L ISO. Left: the black trace depicts the membrane current recorded in control PBS; magenta, in 5.4 mmol/L K^+ 10 mmol/L Cs^+ bathing solution. Right: *I–V* relationship for the HCN2 current (black line) reconstructed from the repolarization phase of the AP clamp experiment in the left panel. The magenta line, recorded in 5.4 mmol/L K^+, 10 mmol/L Cs^+ bathing solution.

the reduction of inward I_h tail current at the membrane potentials more negative than −35 mV [14]. In our earlier report, this phenomenon may have been underestimated because we recorded the APs using the perforated patch method [10]. With that method, the Na^+-Ca^{2+} exchanger current driven by the intracellular Ca^{2+} transient reportedly affects the plateau phase of mouse ventricular APs at around −40 mV and might have masked the prolongation of APD in HCN2-Tg hearts [29]. It should be noted, however, that when the perforated patch method was used in mouse TAC experiments, ventricular I_h density was significantly increased and APD was significantly prolonged [13]. Reduction in repolarization reserve caused by I_h appears to be dependent on the time course of the I_h deactivation upon depolarization. Among the HCN subtypes, the order of the deactivation times at −60 mV was HCN3 > HCN4 > HCN1 > HCN2 [14]. In the present study, even HCN2, which possesses the fastest deactivation time, stayed open during the AP clamp experiments. In the hypertrophied hearts of larger animals, the expression of HCN2 and HCN4 is reportedly up-regulated [30]. Since HCN channels form heteromultimers, it would seem reasonable to expect that the time course of I_h deactivation in hypertrophied hearts would be intermediate, between those of HCN2 and HCN4, and would reduce the repolarization reserve in larger animals, whose cardiac myocytes exhibit longer APDs.

HCN channels reportedly possess Ca^{2+} permeability and re-expression of HCN channels may increase Ca^{2+} influx in hypertrophied heart [16]. The depolarization of RMP may also decrease driving force of Na^+/Ca^{2+} exchanger, thereby increasing intracellular Ca^{2+} concentration. Therefore, the pharmacological blockade of I_h may exert anti-arrhythmogenic effect by maintaining intracellular Ca^{2+} handling as well as repolarization reserve in hypertrophied heart [31].

5. Conclusions

Our findings demonstrate that the transgenic overexpression of HCN2 in the heart induces ectopic automaticity under β-adrenergic stimulation. The overexpression of HCN2 also reduces the repolarization reserve of the AP and prolongs APD. These results suggest that among fetal type cardiac channels re-expressed in heart failure, HCN2 alone is not sufficient to induce lethal arrhythmia, but it increases arrhythmogenic potential. Pharmacological blockade of HCN channels may therefore reduce the vulnerability of heart failure patients to ventricular arrhythmia.

5.1. Limitation of study

Plateau phase of mouse ventricular action potential is at ~−40 mV and is affected by intracellular Ca^{2+} transient. We therefore used Ca^{2+} buffering condition in order to evaluate the change of repolarization reserve in HCN2-Tg myocytes. On the other hand, HCN2 reportedly possesses Ca^{2+} permeability, which may potentially affect intracellular Ca^{2+} transient, giving rise to DADs and ventricular arrhythmia. This arrhythmogenic mechanism may be underestimated in the present study.

Disclosures

None declared.

Acknowledgments

We thank Ms. Hideko Yoshitake and Ms. Akemi Sakamoto for their secretarial work and Ms. Chiemi Sugiyama for her technical support.

This work was supported by a Grant-in-Aid for Scientific Research (B) from the Japan Society for the Promotion of Science (JSPS KAKENHI Grand Number 24300145) and a grant from the Ishibashi Foundation for the Promotion of Science.

Appendix A. Supplementary data

Supplementary data to this article can be found online at http://dx.doi.org/10.1016/j.yjmcc.2014.12.019.

References

[1] Wahl-Schott C, Biel M. HCN channels: structure, cellular regulation and physiological function. Cell Mol Life Sci 2009;66:470–94.
[2] Bucchi A, Baruscotti M, Robinson RB, DiFrancesco D. Modulation of rate by autonomic agonists in SAN cells involves changes in diastolic depolarization and the pacemaker current. J Mol Cell Cardiol 2007;43:39–48.
[3] Yasui K, Liu W, Opthof T, Kada K, Lee JK, Kamiya K, et al. I_f current and spontaneous activity in mouse embryonic ventricular myocytes. Circ Res 2001;88:536–42.
[4] Niwa N, Yasui K, Opthof T, Takemura H, Shimizu A, Horiba M, et al. $Ca_v3.2$ subunit underlies the functional T-type Ca^{2+} channel in murine hearts during the embryonic period. Am J Physiol Heart Circ Physiol 2004;286:H2257–63.
[5] Tomaselli GF, Beuckelmann DJ, Calkins HG, Berger RD, Kessler PD, Lawrence JH, et al. Sudden cardiac death in heart failure. The role of abnormal repolarization. Circulation 1994;90:2534–9.
[6] Nakayama H, Bodi I, Correll RN, Chen X, Lorenz J, Houser SR, et al. α1G-dependent T-type Ca^{2+} current antagonizes cardiac hypertrophy through a NOS3-dependent mechanism in mice. J Clin Invest 2009;119:3787–96.
[7] Wei-qing H, Qing-nuan K, Lin X, Cheng-hao G, Qi-yi Z. Expression of hyperpolarization-activated cyclic nucleotide-gated cation channel (HCN4) is increased in hypertrophic cardiomyopathy. Cardiovasc Pathol 2011;20:110–3.
[8] Fernández-Velasco M, Goren N, Benito G, Blanco-Rivero J, Boscá L, Delgado C. Regional distribution of hyperpolarization-activated current (I_f) and hyperpolarization-activated cyclic nucleotide-gated channel mRNA expression in ventricular cells from control and hypertrophied rat hearts. J Physiol 2003;553:395–405.
[9] Kuwahara K, Saito Y, Takano M, Arai Y, Yasuno S, Nakagawa Y, et al. NRSF regulates the fetal cardiac gene program and maintains normal cardiac structure and function. EMBO J 2003;22:6310–21.
[10] Kuwabara Y, Kuwahara K, Takano M, Kinoshita H, Arai Y, Yasuno S, et al. Increased expression of HCN channels in the ventricular myocardium contributes to enhanced arrhythmicity in mouse failing hearts. J Am Heart Assoc 2013;2:e000150-e.
[11] Oshita K, Igata S, Kuwabara Y, Kuwahara K, Ushijima K, Takano M. Isoproterenol-induced spontaneous action potentials in the cardiac myocytes of transgenic mouse overexpressing HCN2. J Physiol Sci 2013;63:S134.
[12] Takano M, Kinoshita H, Shioya T, Itoh M, Nakao K, Kuwahara K. Pathophysiological remodeling of mouse cardiac myocytes expressing dominant negative mutant of neuron restrictive silencing factor. Circ J 2010;74:2712–9.
[13] Hofmann F, Fabritz L, Stieber J, Schmitt J, Kirchhof P, Ludwig A, et al. Ventricular HCN channels decrease the repolarization reserve in the hypertrophic heart. Cardiovasc Res 2012;95:317–26.
[14] Fenske S, Mader R, Scharr A, Paparizos C, Cao-Ehlker X, Michalakis S, et al. HCN3 contributes to the ventricular action potential waveform in the murine heart. Circ Res 2011;109:1015–23.
[15] Kapoor N, Liang W, Marbán E, Cho HC. Direct conversion of quiescent cardiomyocytes to pacemaker cells by expression of Tbx18. Nat Biotechnol 2013;31:54–62.
[16] Yu X, Chen X-W, Zhou P, Yao L, Liu T, Zhang B, et al. Calcium influx through I_f channels in rat ventricular myocytes. Am J Physiol Cell Physiol 2007;292:1147–55.
[17] Stillitano F, Lonardo G, Zicha S, Varro A, Cerbai E, Mugelli A, et al. Molecular basis of funny current (I_f) in normal and failing human heart. J Mol Cell Cardiol 2008;45:289–99.
[18] Hoppe UC, Jansen E, Südkamp M, Beuckelmann DJ. Hyperpolarization-activated inward current in ventricular myocytes from normal and failing human hearts. Circulation 1998;97:55–65.
[19] Jaleel N, Nakayama H, Chen X, Kubo H, MacDonnell S, Zhang H, et al. Ca^{2+} influx through T- and L-type Ca^{2+} channels have different effects on myocyte contractility and induce unique cardiac phenotypes. Circ Res 2008;103:1109–19.
[20] Boink GJJ, Duan L, Nearing BD, Shlapakova IN, Sosunov EA, Anyukhovsky EP, et al. HCN2/SkM1 gene transfer into canine left bundle branch induces stable, autonomically responsive biological pacing at physiological heart rates. J Am Coll Cardiol 2013;61:1192–201.
[21] Kinoshita H, Kuwahara K, Takano M, Arai Y, Kuwabara Y, Yasuno S, et al. T-type Ca^{2+} channel blockade prevents sudden death in mice with heart failure. Circulation 2009;120:743–52.
[22] Galindo CL, Skinner MA, Errami M, Olson LD, Watson DA, Li J, et al. Transcriptional profile of isoproterenol-induced cardiomyopathy and comparison to exercise-induced cardiac hypertrophy and human cardiac failure. BMC Physiol 2009;9:23.
[23] Adachi T, Shibata S, Okamoto Y, Sato S, Fujisawa S, Ohba T, et al. The mechanism of increased postnatal heart rate and sinoatrial node pacemaker activity in mice. J Physiol Sci 2013;63:133–46.
[24] Nerbonne JM, Kass RS. Molecular physiology of cardiac repolarization. Physiol Rev 2005;85:1205–53.
[25] Ishihara K, Yan DH, Yamamoto S, Ehara T. Inward rectifier K^+ current under physiological cytoplasmic conditions in guinea-pig cardiac ventricular cells. J Physiol 2002;540:831–41.
[26] Babij P, Askew GR, Nieuwenhuijsen B, Su CM, Bridal TR, Jow B, et al. Inhibition of cardiac delayed rectifier K^+ current by overexpression of the long-QT syndrome HERG G628S mutation in transgenic mice. Circ Res 1998;83:668–78.

[27] Nattel S, Maguy A, Le Bouter S, Yeh YH. Arrhythmogenic ion-channel remodeling in the heart: heart failure, myocardial infarction, and atrial fibrillation. Physiol Rev 2007;87:425–56.
[28] Varró A, Baczkó I. Cardiac ventricular repolarization reserve: a principle for understanding drug-related proarrhythmic risk. Br J Pharmacol 2011;164:14–36.
[29] Wang J, Chan TO, Zhang XQ, Gao E, Song J, Koch WJ, et al. Induced overexpression of Na^+/Ca^{2+} exchanger transgene: altered myocyte contractility, $[Ca^{2+}]_i$ transients, SR Ca^{2+} contents, and action potential duration. Am J Physiol Heart Circ Physiol 2009; 297:H590–601.
[30] Herrmann S, Stieber J, Ludwig A. Pathophysiology of HCN channels. Pflugers Arch 2007;454:517–22.
[31] Swedberg K, Komajda M, Böhm M, Borer JS, Ford I, Dubost-Brama A, et al. Ivabradine and outcomes in chronic heart failure (SHIFT): a randomised placebo-controlled study. Lancet 2010;376:875–85.

Cardiovascular Research (2014) **104**, 183–193
doi:10.1093/cvr/cvu185

Inhibition of N-type Ca^{2+} channels ameliorates an imbalance in cardiac autonomic nerve activity and prevents lethal arrhythmias in mice with heart failure

Yuko Yamada[1,2†], Hideyuki Kinoshita[1,3†], Koichiro Kuwahara[1,3*], Yasuaki Nakagawa[1,3], Yoshihiro Kuwabara[1,4], Takeya Minami[1,3], Chinatsu Yamada[1,3], Junko Shibata[1,3], Kazuhiro Nakao[1,2,3], Kosai Cho[3,5], Yuji Arai[6], Shinji Yasuno[4], Toshio Nishikimi[1,3], Kenji Ueshima[4], Shiro Kamakura[7], Motohiro Nishida[8], Shigeki Kiyonaka[9], Yasuo Mori[9], Takeshi Kimura[3], Kenji Kangawa[2,10], and Kazuwa Nakao[1,11]

[1]Department of Medicine and Clinical Science, Kyoto University Graduate School of Medicine, 54 Shogoin Kawaharacho, Sakyo-ku, Kyoto 606-8507, Japan; [2]Department of Peptide Research, Kyoto University Graduate School of Medicine, Kyoto 606-8507, Japan; [3]Department of Cardiovascular Medicine, Kyoto University Graduate School of Medicine, Kyoto 606-8507, Japan; [4]Department of EBM Research, Institute for Advanced of Clinical and Translational Science, Kyoto University Hospital, Kyoto 606-8507, Japan; [5]Department of Primary Care and Emergency Medicine, Kyoto University Graduate School of Medicine, Kyoto 606-8507, Japan; [6]Department of Bioscience and Genetics, National Cerebral and Cardiovascular Center Research Institute, Suita 565-8565, Japan; [7]Department of Cardiovascular Medicine, National Cerebral and Cardiovascular Center, Suita 565-8565, Japan; [8]Division of Cardiocirculatory Signaling, Okazaki Institute for Integrative Bioscience (National Institute for Physiological Sciences), National Institute for Natural Sciences, Aichi 444-8787, Japan; [9]Department of Synthetic Chemistry and Biological Chemistry, Kyoto University Graduated School of Engineering, Kyoto 615-8530, Japan; [10]Department of Biochemistry, National Cerebral and Cardiovascular Center Research Institute, Suita 606-8507, Japan; and [11]Medical Innovation Center, Kyoto University Graduate School of Medicine, Kyoto 606-8507, Japan

Received 21 January 2014; revised 24 July 2014; accepted 30 July 2014; online publish-ahead-of-print 5 August 2014

Time for primary review: 10 days

Aims Dysregulation of autonomic nervous system activity can trigger ventricular arrhythmias and sudden death in patients with heart failure. N-type Ca^{2+} channels (NCCs) play an important role in sympathetic nervous system activation by regulating the calcium entry that triggers release of neurotransmitters from peripheral sympathetic nerve terminals. We have investigated the ability of NCC blockade to prevent lethal arrhythmias associated with heart failure.

Methods and results We compared the effects of cilnidipine, a dual N- and L-type Ca^{2+} channel blocker, with those of nitrendipine, a selective L-type Ca^{2+} channel blocker, in transgenic mice expressing a cardiac-specific, dominant-negative form of neuron-restrictive silencer factor (dnNRSF-Tg). In this mouse model of dilated cardiomyopathy leading to sudden arrhythmic death, cardiac structure and function did not significantly differ among the control, cilnidipine, and nitrendipine groups. However, cilnidipine dramatically reduced arrhythmias in dnNRSF-Tg mice, significantly improving their survival rate and correcting the imbalance between cardiac sympathetic and parasympathetic nervous system activity. A β-blocker, bisoprolol, showed similar effects in these mice. Genetic titration of NCCs, achieved by crossing dnNRSF-Tg mice with mice lacking *CACNA1B*, which encodes the α1 subunit of NCCs, improved the survival rate. With restoration of cardiac autonomic balance, dnNRSF-Tg;*CACNA1B*$^{+/-}$ mice showed fewer malignant arrhythmias than dnNRSF-Tg;*CACNA1B*$^{+/+}$ mice.

Conclusions Both pharmacological blockade of NCCs and their genetic titration improved cardiac autonomic balance and prevented lethal arrhythmias in a mouse model of dilated cardiomyopathy and sudden arrhythmic death. Our findings suggest that NCC blockade is a potentially useful approach to preventing sudden death in patients with heart failure.

Keywords Ion channel • Nervous system • Autonomic • Heart failure • Arrhythmia • N-type Ca^{2+} channel

* Corresponding author. Tel: +81 75 751 4287; fax: +81 75 771 9452. E-mail: kuwa@kuhp.kyoto-u.ac.jp

† These authors contributed equally to this work.

1. Introduction

Approximately 50% of deaths among patients with heart failure are classified as sudden death, mainly caused by lethal arrhythmias.[1] Despite recent progress, pharmacological interventions for the treatment and prevention of lethal arrhythmias associated with chronic heart failure remain unsatisfactory. Nonetheless, it is anticipated that a better understanding of the molecular basis of arrhythmicity in failing hearts will enable identification of therapeutic targets that can serve as the basis for the development of new pharmacological treatments.

Autonomic dysregulation leading to increased sympathetic nerve activity and decreased parasympathetic nerve activity contributes to the increased arrhythmicity seen in patients with chronic heart failure.[2,3] N-type voltage-dependent Ca^{2+} channels (NCCs), encoded by the *CACNA1B* (α1B subunit) gene, are predominantly localized in the nervous system, where they play a pivotal role in modulating a variety of neuronal functions, including neurotransmitter release at sympathetic nerve terminals.[4–6] Mice lacking *CACNA1B* show functional deterioration of their sympathetic nervous system,[7] and the ability of NCC blockade to prevent malignant arrhythmias and sudden death associated with heart failure remains unevaluated.

We previously reported that transgenic mice cardiac-selectively expressing a dominant-negative form of neuron-restrictive silencer factor (NRSF, also called REST) (dnNRSF-Tg), a transcriptional repressor important for regulation of the fetal cardiac gene program, showed progressive cardiomyopathy and sudden arrhythmic death beginning at about 8 weeks of age.[8] We have also reported several abnormalities in cardiac electrophysiological properties and ion channel expression in these dnNRSF-Tg mice.[9,10] The dnNRSF-Tg hearts showed increased expression of fetal-type ion channel genes, including *CACNA1H*, which encodes the T-type Ca^{2+} channel (TCC) α1 subunit, and a corresponding increase in $I_{ca,T}$ amplitude.[8] In that earlier study, we demonstrated that TCC blockade could prevent sudden death in dnNRSF-Tg mice by both restoring the normal electrophysiology of ventricular myocytes and correcting the cardiac autonomic dysfunction observed in dnNRSF-Tg mice.[11] Because TCC expression, and thus functional TCC currents, is increased in the myocardium of dnNRSF-Tg mice, TCC blockade directly affects the electrophysiological properties of ventricular myocytes in dnNRSF-Tg mice. On the other hand, the impact of modulating autonomic nervous system balance on the incidence of lethal arrhythmias in dnNRSF-Tg mice remains unclear.

Pharmacological blockade or genetic deletion of NCCs reportedly alters autonomic activity in both human patients and animal models.[7,12,13] On the other hand, little or no NCC expression has been detected in the ventricular myocardium. Therefore, to evaluate the extent to which correcting the autonomic imbalance prevents the lethal arrhythmias associated with heart failure, we assessed the effects of pharmacological blockade of NCCs and their genetic titration on arrhythmicity and sudden death in dnNRSF-Tg mice. Our findings demonstrate the importance of an imbalance between sympathetic and parasympathetic nerve activities in the generation of lethal arrhythmias in failing hearts and suggest that restoring autonomic nervous system balance through NCC inhibition can be an effective approach to preventing sudden arrhythmic death associated with heart failure.

2. Methods

An expanded Methods section is available in Supplementary material online.

2.1 Animal experiments

The animal care and all experimental protocols were reviewed and approved by the Animal Research Committee at Kyoto University Graduate School of Medicine, and conformed to the US National Institute of Health Guide for the Care and Use of Laboratory Animals. Beginning at 8 weeks of age, dnNRSF-Tg mice were left untreated (control) or were treated for 24 weeks with cilnidipine (10 mg/kg/day po) or nitrendipine (10 mg/kg/day po). The drug dosages were chosen based on earlier reports and our preliminary studies.[14,15] Cilnidipine was supplied by Mochida Pharmaceutical Co., Ltd (Tokyo, Japan). Nitrendipine was purchased from Wako Pure Chemical Industries, Ltd (Osaka, Japan). Bisoprolol was supplied by Mitsubishi Tanabe Pharma Corporation (Osaka, Japan). Cilnidipine exerts a much more potent inhibitory effect on N-type Ca^{2+} currents than does nitrendipine, which has little effect on N-type Ca^{2+} currents, particularly under conditions in which L-type Ca^{2+} current inhibition is comparable between the two drugs.[16,17] We then selected the doses of both drugs that similarly and minimally affected blood pressure. In another experiment, dnNRSF-Tg mice were bred with *CACNA1B* heterozygous knockout mice to obtain dnNRSF-Tg; $CACNA1B^{+/-}$ mice and control dnNRSF-Tg;$CACNA1B^{+/+}$ littermates. $CACNA1B^{+/-}$ mice were described in an earlier report.[7] For the isolation and analysis of hearts, mice were anaesthetized with 3.0% of isoflurane and sacrificed by cervical dislocation.

2.2 Statistical analysis

Data are presented as means ± standard errors of the mean (SEM) unless indicated otherwise. Survival was analysed using the Kaplan–Meier method with the log-rank test. Comparisons among multiple groups were made using ANOVA with post hoc Fisher's tests, except for numbers of arrhythmias. Values of $P < 0.05$ were considered significant. Numbers of arrhythmias between two groups were analysed using the Mann–Whitney test. Values of $P < 0.05$ were considered significant. Numbers of arrhythmias among four groups were analysed using Kruskal–Wallis non-parametric ANOVA followed by the Bonferroni correction. Values of $P < 0.0083$ were considered significant in that analysis.

3. Results

3.1 The dual N- and L-type Ca^{2+} channel blocker cilnidipine improves survival among dnNRSF-Tg mice without affecting cardiac structure or function

We initially confirmed that there is little expression of *CACNA1B*, encoding the α1 subunit of NCCs, in either wild-type (WT) or dnNRSF-Tg hearts, which is in contrast to its obvious expression in brain (*Figure 1A*). On the other hand, we detected substantially greater ventricular expression of *CACNA1H*, encoding the α1 subunit of TCCs, and *CACNA1C*, encoding the α1 subunit of L-type Ca^{2+} channels (*Figure 1B*). Although ventricular expression of *CACNA1B* is increased in dnNRSF-Tg hearts, probably due to the presence of NRSF-binding element in the gene, the levels are still lower than those of *CACNA1H* in WT hearts, where no functional T-type Ca^{2+}currents are detected.[11,18] To evaluate the potential therapeutic effect of modulating autonomic nervous system activity through NCC blockade on the development of malignant arrhythmias and sudden death in dnNRSF-Tg mice, we administered subpressor doses of cilnidipine, a dual N- and L-type dihydropyridine Ca^{2+} channel blocker, or nitrendipine, a more L-type-selective dihydropyridine Ca^{2+} channel blocker, to dnNRSF-Tg mice for 24 weeks, beginning when they were 8 weeks of age. Under our experimental conditions, systolic blood pressures and heart rates did not differ among the control, cilnidipine, and nitrendipine groups

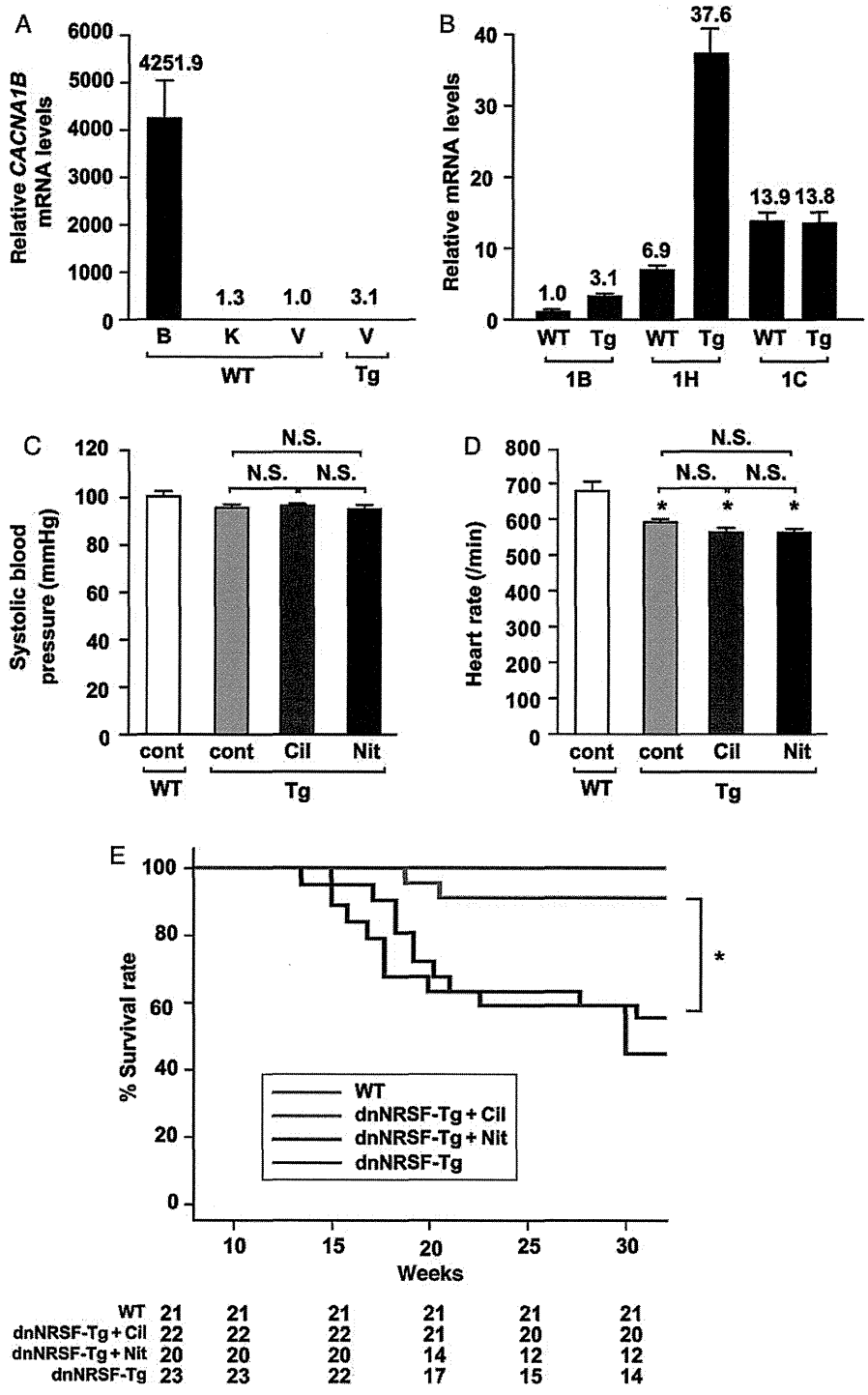

Figure 1 Pharmacological blockade of NCCs by cilnidipine improves survival among dnNRSF-Tg mice. (*A*) Relative levels of CACNA1B mRNA in brains (B) from WT, kidney (K) from WT, cardiac ventricle (V) from WT, and cardiac ventricle (V) from 8-week-old dnNRSF-Tg mice (Tg); levels in cardiac ventricle from WT mice were assigned a value of 1.0. $n = 3$ each for brain, kidney, and cardiac ventricle from WT mice and $n = 2$ for cardiac ventricle from dnNRSF-Tg mice. (*B*) Relative levels of CACNA1B, CACNA1H, and CACNA1C mRNA in cardiac ventricle from 8-week-old WT mice and dnNRSF-Tg mice (Tg); levels of CACNA1B mRNA in WT mice were assigned a value of 1.0. $n = 5$ for WT mice and $n = 7$ for dnNRSF-Tg. (*C* and *D*) Systolic blood pressures (*C*) and heart rates (*D*) in 20-week-old untreated WT, untreated Tg (Tg-cont), cilnidipine-treated Tg (Tg-Cil), and nitrendipine-treated Tg-Nit mice ($n = 15$ each for untreated Tg, Tg-Cil, and Tg-Nit, and $n = 10$ for untreated WT). ANOVA with post hoc Fisher's tests was used for analysis. *$P < 0.05$. N.S.: not significant. (*E*) Kaplan–Meyer survival curves for untreated WT, untreated Tg, Cil-treated Tg, and Nit-treated Tg over a 24-week drug administration period (from 8 to 32 weeks of age): Log-rank test was used for analysis. *$P < 0.05$ ($n = 21$ for WT, $n = 23$ for Tg without drugs, $n = 22$ for Tg + Cil, and $n = 20$ for Tg + Nit). The numbers of mice alive in each group at the end of each period are shown at the bottom of the figure. All data except survival curves are shown as means ± SEM.

of dnNRSF-Tg mice, though blood pressures were slightly lower and heart rates were significantly slower in dnNRSF-Tg mice than in untreated WT mice, as previously reported (systolic blood pressure: WT, 101.40 ± 1.48; Tg, 96.0 ± 1.75; Tg + cilnidipine, 96.67 ± 1.64; Tg + nitrendipine, 95.47 ± 1.92 mmHg and Heart rates: WT, 682.3 ± 27; dnNRSF-Tg, 590.6 ± 10.9; Tg + cilnidipine, 567.13 ± 17.58; Tg + nitrendipine, 568.8 ± 11.07/min) (*Figure 1C* and *D*).[8] We found that cilnidipine dramatically improved the survival rate among dnNRSF-Tg mice, compared with mice treated with nitrendipine or untreated control (*Figure 1E*). Although heart-to-body weight ratios were higher in dnNRSF-Tg than in WT mice, as reported previously,[8] heart-to-body weight ratios did not significantly differ among the control, cilnidipine, and nitrendipine groups of dnNRSF-Tg mice (WT, 4.08 ± 0.31; Tg, 5.94 ± 0.24; Tg + cilnidipine, 5.61 ± 0.48; Tg + nitrendipine, 5.94 ± 0.36 mg/g) (*Figure 2A*). Lung-to-body weight ratios also did not differ among these three groups (WT, 5.28 ± 0.37; Tg, 6.07 ± 0.22; Tg + cilnidipine, 5.93 ± 0.79; Tg + nitrendipine, 5.9 ± 0.29 mg/g) (*Figure 2B*). In addition, histological analyses, including determination of the %fibrotic area, and echocardiographic analyses also showed no significant differences among these three groups (*Figure 2C–F* and *Table 1*). In contrast, the echocardiography and histology showed that, compared with untreated WT mice, left ventricular systolic function was diminished and %fibrotic area was increased in dnNRSF-Tg mice, as reported previously (*Figure 2C–F* and *Table 1*).[8] Consistent with these findings, there was no significant difference in the expression of two cardiac stress marker genes, *ANP* and *SERCA2*, among the three groups, whereas their expression did differ between untreated WT mice and dnNRSF-Tg mice, as described previously (*Figure 2G* and *H*).[8]

Expression of the fibrosis-related genes *Col1a1*, *Col3a1*, and *FN1*, encoding collagen type1α1, collagen type3α1, and fibronectin 1, respectively, was not affected by the drug treatments (see Supplementary material online, *Figure S1A–C*). Expression of genes encoding the fetal-type ion channels *CACNA1H*, *HCN2*, and *HCN4* was higher in untreated dnNRSF-Tg ventricles than in control WT ventricles, as reported previously, and cilnidipine did not affect expression of these genes in dnNRSF-Tg ventricles (see Supplementary material online, *Figure S1D–F*). Collectively, all of these data indicate that cilnidipine suppresses sudden death in dnNRSF-Tg mice without significantly affecting cardiac structure or function.

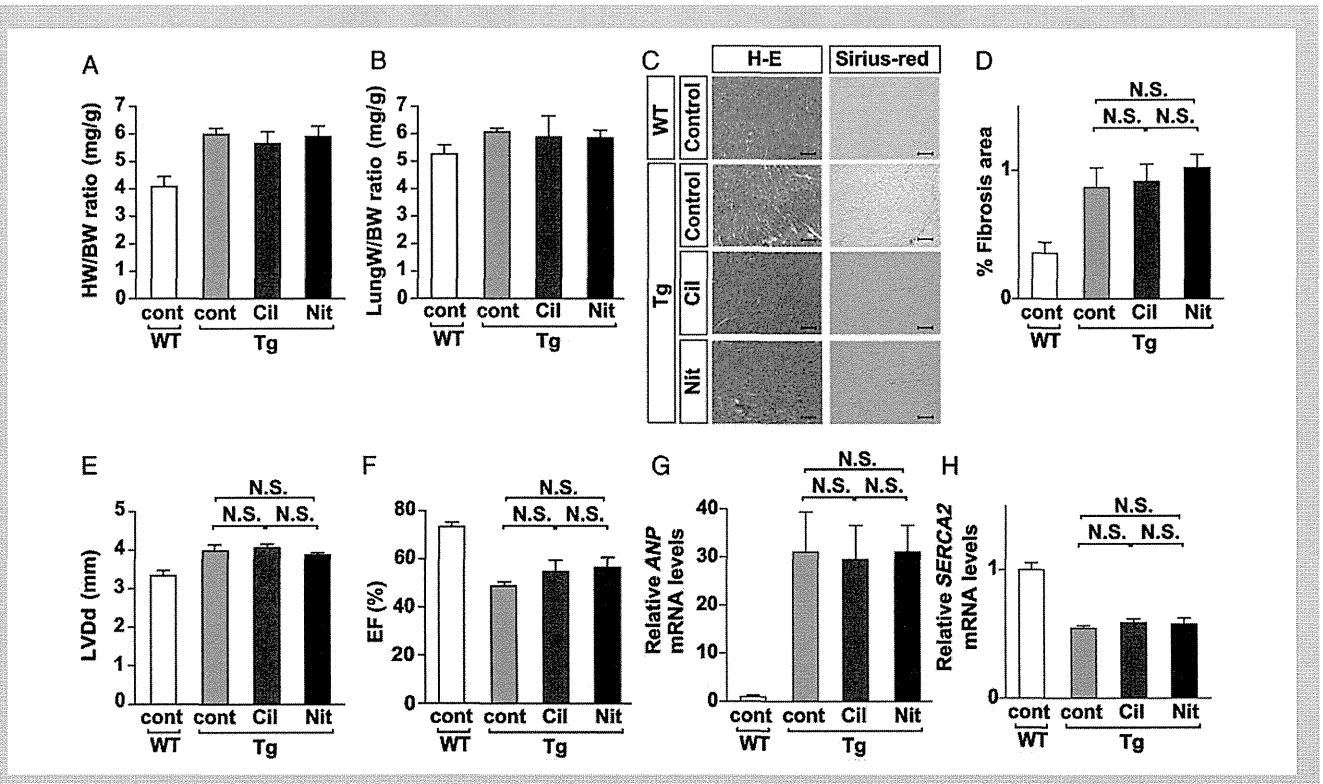

Figure 2 Cilnidipine does not affect cardiac structure or function in dnNRSF-Tg mice. (*A* and *B*) Heart-to-body weight (HW/BW) ratios (*A*) and lung-to-body weight (LungW/BW) ratios (*B*) in 20-week-old untreated WT (WT-cont), untreated Tg (Tg-cont), Cil-treated Tg (Tg-Cil), and Nit-treated Tg (Tg-Nit) mice ($n = 5$ for untreated WT, $n = 4$ for Tg-cont, $n = 4$ for Tg-Cil, and $n = 3$ for Tg-Nit). (*C*) Histology of hearts from 20-week-old untreated WT, Tg-cont, Tg-Cil, and Tg-Nit mice: H-E, haematoxylin-eosin staining; Sirius-red, Sirius-red staining. Scale bars = 100 μm. (*D*) %fibrotic area in 20-week-old untreated WT, Tg-cont, Tg-Cil, and Tg-Nit mice ($n = 5$ for Tg-cont; $n = 7$ for Tg-Cil). N.S.: not significant. (*E* and *F*) LVDd (*E*) and EF (*F*) assessed echocardiographically in untreated WT, Tg-cont, Tg-Cil, and Tg-Nit mice. *$P < 0.05$. N.S.: not significant. ($n = 5$ each for untreated WT, Tg-cont, and Tg-Cil; $n = 7$ for Tg-Nit). (*G* and *H*) Relative levels of ANP (*G*) and SERCA2 (*H*) mRNA in cardiac ventricles from untreated WT, Tg-cont, Tg-Cil, and Tg-Nit mice; levels in untreated WT were assigned a value of 1.0. N.S.: not significant. ($n = 4$ each). ANOVA with post hoc Fisher's tests was used for analysis. All data are shown as means ± SEM.

Table 1 Echocardiographic parameters in 20-week-old mice

	WT	dnNRSF-Tg		
	Control	Cont	Cil	Nit
Pharmacological inhibition				
LVDd (mm)	3.3 ± 0.13	3.9 ± 0.19	4.0 ± 0.11	3.8 ± 0.08
LVDs (mm)	2.1 ± 0.08	3.1 ± 0.17	3.1 ± 0.11	2.9 ± 0.10
IVST (mm)	0.76 ± 0.02	0.72 ± 0.02	0.72 ± 0.02	0.71 ± 0.03
PWT (mm)	0.76 ± 0.02	0.74 ± 0.02	0.76 ± 0.02	0.76 ± 0.03
FS (%)	36.1 ± 2.3	20.3 ± 1.4	23.3 ± 2.7	23.8 ± 2.4
EF (%)	73.2 ± 2.7	49.0 ± 2.3	55.4 ± 4.2	57.0 ± 4.3
			dnNRSF-Tg	
	$1B^{+/+}$	$1B^{+/-}$	$1B^{+/+}$	$1B^{+/-}$
Genetic titration				
LVDd (mm)	3.2 ± 0.10	3.3 ± 0.08	4.1 ± 0.12	3.3 ± 0.07*
LVDs (mm)	2.2 ± 0.12	2.2 ± 0.06	3.2 ± 0.13	2.3 ± 0.08*
IVST (mm)	0.66 ± 0.01	0.68 ± 0.02	0.66 ± 0.02	0.69 ± 0.02
PWT (mm)	0.68 ± 0.02	0.67 ± 0.02	0.66 ± 0.02	0.68 ± 0.02
FS (%)	31.8 ± 1.8	33.1 ± 1.9	20.4 ± 1.3	30.4 ± 1.3*
EF (%)	66.4 ± 2.4	68.9 ± 2.6	49.0 ± 2.4	64.3 ± 1.8*

Values are means ± SEM. Cil, cilnidipine; Nit, nitrendipine; $1B^{+/+}$, $CACNA1B^{+/+}$; $1B^{+/-}$, $CACNA1B^{+/-}$; LVDd, left ventricular diastolic dimension; LVDs, left ventricular systolic dimension; FS, fractional shortening; IVST, intraventricular septum wall thickness; PWT, posterior wall thickness. Numbers of mice tested in the pharmacological inhibition study are as follows: $n = 5$ for WT, untreated dnNRSF-Tg, and Cil-treated dnNRSF-Tg; $n = 7$ for Nit-treated dnNRSF-Tg (upper panel). Numbers of mice tested in the genetic titration study are as follows: $n = 13$ for $1B^{+/+}$, $n = 14$ for $1B^{+/-}$, $n = 11$ for dnNRSF-Tg;$1B^{+/+}$, and $n = 15$ for dnNRSF-Tg; $1B^{+/-}$ (lower panel). ANOVA with *post hoc* Fisher's tests was used for the analysis.
*$P < 0.05$ vs. dnNRSF-Tg;$1B^{+/+}$.

3.2 Cilnidipine improves cardiac autonomic nervous system function and reduces arrhythmicity in dnNRSF-Tg mice

We hypothesized that correcting autonomic balance through NCC blockade reduces arrhythmogenicity, thereby improving survival among dnNRSF-Tg mice. Heart rate variability (HRV) is a widely accepted index of cardiac autonomic nervous system activity.[19] Earlier frequency domain analysis of HRV revealed that patients with severe heart failure show a progressive reduction in power in both the low-frequency (LF) and high-frequency (HF) ranges,[19] and that a reduction in the LF power range is a significant predictor of sudden cardiac death in patients with heart failure.[20] We used HRV as an index to evaluate cardiac autonomic function in WT and dnNRSF-Tg mice, and examined the effects of cilnidipine on HRV.[19] In mice, HRV predominantly correlates with parasympathetic activity.[21] As we showed previously, both the LF and HF powers averaged over 24 h in dnNRSF-Tg mice (LF, 1.228 ± 0.198; HF, 0.823 ± 0.186 m/s^2) were markedly lower than in WT mice (LF, 4.331 ± 0.706; HF, 2.412 ± 0.089 m/s^2), indicating a general reduction in parasympathetic activity in dnNRSF-Tg mice (*Figure 3A* and *B*). Cilnidipine dramatically increased the power in both the LF and HF ranges of HRV (LF, 3.308 ± 0.338; HF, 2.228 ± 0.283 m/s^2), whereas nitrendipine had little effect on HRV (LF, 0.538 ± 0.447; HF, 1.383 ± 0.57 m/s^2) (*Figure 3A* and *B*). We also found that urinary excretion of norepinephrine, which is indicative of the level of sympathetic nerve activity, was significantly higher in dnNRSF-Tg than in WT mice, and that norepinephrine excretion was significantly reduced only by cilnidipine (WT, 0.09 ± 0.02; Tg, 0.33 ± 0.04; Tg + cilnidipine, 0.15 ± 0.03; Tg + nitrendipine, 0.32 ± 0.1 μg/day) (*Figure 3C*).

We next used an implanted telemetric monitoring system to examine the effects of cilnidipine and nitrendipine on electrocardiographic parameters in dnNRSF-Tg mice. We found that only cilnidipine significantly suppressed the number of premature ventricular contractions (PVCs) in dnNRSF-Tg hearts (WT, 0 ± 0; dnNRSF-Tg, 502.66 ± 305.69; dnNRSF-Tg + cilnidipine, 1.0 ± 0.66; dnNRSF-Tg + nitrendipine, 326.17 ± 147.24 /h) (*Figure 3D*). More importantly, it dramatically reduced the number of episodes of ventricular tachycardia (VT) (WT, 0 ± 0; dnNRSF-Tg, 14.92 ± 4.95; dnNRSF-Tg + cilnidipine, 0.06 ± 0.06; dnNRSF-Tg + nitrendipine, 12.75 ± 5.16/h) (*Figure 3E* and Supplementary material online, *Figure S2A* and *B*). These lines of evidence suggest that by restoring autonomic nervous system balance, cilnidipine reduces the incidence of lethal arrhythmias in dnNRSF-Tg mice.

3.3 β-Adrenergic receptor blockade prevents lethal arrhythmias and sudden death in dnNRSF-Tg mice

To verify the importance of correcting autonomic nervous system imbalance for the prevention of lethal arrhythmias and sudden death in dnNRSF-Tg mice, irrespective of effects on structural remodelling, we examined the effects of treating these mice with a β-adrenergic receptor blocker. We administered a subpressor dose of the lipophilic β-adrenergic receptor blocker bisoprolol (1 mg/kg/day po) to WT and dnNRSF-Tg mice. Although systolic blood pressures did not differ between untreated control and bisoprolol-treated mice (untreated WT, 107.5 ± 1.6; WT + bisoprolol, 108.0 ± 1.2; untreated Tg, 98.6 ± 2.0; Tg + bisoprolol, 98.6 ± 1.7 mmHg) (*Figure 3F*), heart rates were significantly slower in bisoprolol-treated than in untreated WT and dnNRSF-Tg mice (untreated WT, 697.8 ± 8.3; WT + bisoprolol,

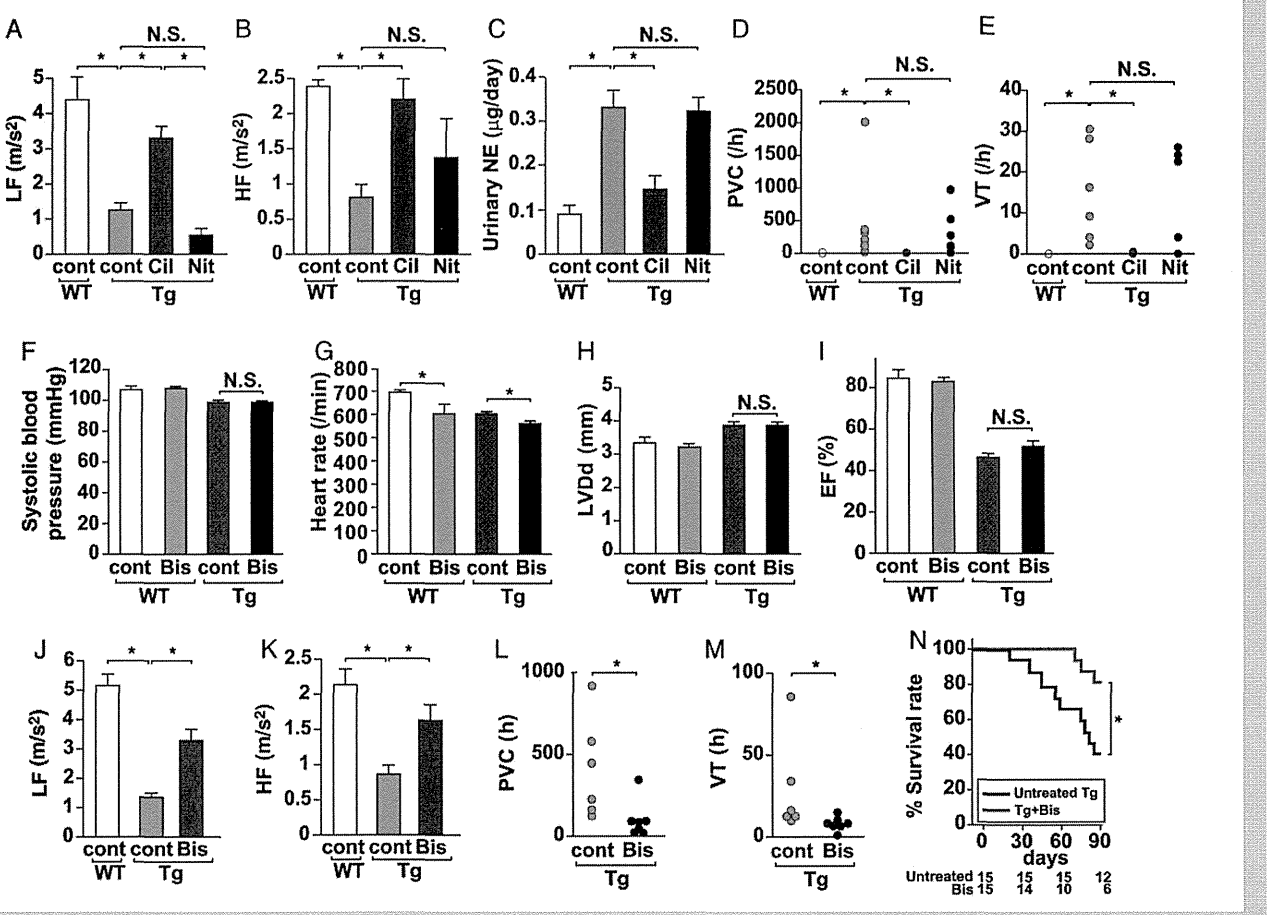

Figure 3 Cilnidipine restores cardiac autonomic nervous system balance and reduces arrhythmias in dnNRSF-Tg mice. (*A* and *B*) Average power of the LF (*A*) and HF (*B*) components of HRV recorded over a 24-h period in 20-week-old untreated WT (WT-cont), untreated Tg (Tg-cont), Cil-treated Tg (Tg-Cil), and Nit-treated (Tg-Nit) mice. $^*P < 0.05$. N.S.: not significant ($n = 5$ for WT, $n = 6$ for Tg-cont, $n = 8$ for Tg-Cil, and $n = 6$ for Tg-Nit). (*C*) Urinary norepinephrine (NE) levels in 20-week-old WT-cont, Tg-cont, Tg-Cil, and Tg-Nit mice. $^*P < 0.05$. N.S.: not significant ($n = 7$ for WT, $n = 7$ for Tg-cont, $n = 5$ for Tg-Cil, and $n = 4$ for Tg-Nit). (*D* and *E*) Numbers of PVC (*D*) and VT (*E*) recorded with a telemetry system in 20-week-old WT-cont, Tg-cont, Tg-Cil, and Tg-Nit mice are shown by dot plots. $^*P < 0.0083$, N.S.: not significant ($n = 5$ for WT-cont, $n = 6$ for Tg-cont, $n = 8$ for Tg-Cil, and $n = 6$ for Tg-Nit). (*F* and *G*) Systolic blood pressures (*F*) and heart rates (*G*) in 20-week-old untreated WT (WT-cont), bisoprolol (Bis)-treated WT (WT-Bis), untreated Tg (Tg-cont), and Bis-treated Tg (Tg-Bis) mice ($n = 4$ for WT-cont, $n = 3$ for WT-Bis, and $n = 5$ for Tg-cont and Tg-Bis). (*H* and *I*) LVDd (*H*) and EF (*I*) assessed echocardiographically in WT-cont, WT-Bis, Tg-cont, and Tg-Bis mice. $^*P < 0.05$. N.S.: not significant. ($n = 4$ for WT-cont, $n = 3$ for WT-Bis, and $n = 5$ for Tg-cont and Tg-Bis). (*J* and *K*) Average power of the LF (*J*) and HF (*K*) components of heart rate variability (HRV) recorded over a 24-h period in 20-week-old WT-cont, Tg-cont, and Tg-Bis mice. $^*P < 0.05$. N.S.: not significant ($n = 4$ for WT-cont, $n = 6$ for Tg-cont, and $n = 7$ for Tg-Bis). (*L* and *M*) Numbers of PVC (*L*) and VT (*M*) recorded with a telemetry system in 20-week-old Tg-cont and Tg-Bis mice are shown by dot plots. $^*P < 0.05$ ($n = 6$ for Tg-cont; $n = 7$ for Tg-Bis). ANOVA with post hoc Fisher's tests was used for analysis, except for numbers of arrhythmias (*D*, *E*, *L*, and *M*). Numbers of arrhythmias among the four groups were analyzed using Kruskal–Wallis non-parametric ANOVA followed by the Bonferroni correction (*D* and *E*). Numbers of arrhythmias between two groups were analyzed using non-parametric Mann–Whitney test (*L* and *M*). (*N*) Kaplan–Meyer survival curves for untreated Tg and Bis-treated Tg (Tg + Bis) over a 90-day drug administration period (from 12 to 25 weeks of age): Log-rank test was used for the survival analysis. $^*P < 0.05$ ($n = 15$ each). The numbers of mice alive in each group at the end of each period are shown at the bottom of the figure. All data except numbers of arrhythmias and survival curves are shown as means ± SEM.

604.7 ± 38.3; Tg, 601.6 ± 10.1; Tg + bisoprolol, 558.6 ± 12.0/min) (*Figure 3G*). At the dose tested, bisoprolol also did not affect cardiac systolic function assessed echocardiographically in dnNRSF-Tg mice [LVDd: WT, 3.3 ± 0.2; WT + bisoprolol, 3.2 ± 0.1; Tg, 3.9 ± 0.1; Tg + bisoprolol, 3.9 ± 0.1 mm and ejection fraction (EF): WT, 84.5 ± 4.0; WT + bisoprolol, 83.0 ± 1.5; Tg, 46.0 ± 1.6; Tg + bisoprolol, 51.5 ± 2.7%] (*Figure 3H* and *I*). On the other hand, bisoprolol significantly restored power in both the LF and HF ranges of HRV (LF: untreated WT, 5.19 ± 0.37; Tg, 1.36 ± 0.14; Tg + bisoprolol, 3.34 ± 0.39 m/s^2 and HF: untreated WT, 2.12 ± 0.24; Tg, 0.86 ± 0.12; Tg + bisoprolol, 1.62 ± 0.22 m/s^2) (*Figure 3J* and *K*) and reduced the incidence of PVCs and VTs in those mice (PVC: Tg, 408.3 ± 122.9; Tg + bisoprolol, 98.9 ± 42.2/h; VT: Tg, 28.2 ± 12.1; Tg + bisoprolol, 7.6 ± 1.7/h) (*Figure 3L* and *M*). As a result, bisoprolol significantly improved survival rates among dnNRSF-Tg mice (*Figure 3N*). These results strongly support our finding that imbalance of autonomic nervous system

activities is critically involved in the occurrence of sudden arrhythmic death in dnNRSF-Tg mice.

3.4 Genetic titration of NCC improves survival among dnNRSF-Tg mice

To further confirm the benefit of NCC inhibition for prevention of sudden death in dnNRSF-Tg mice, we next genetically titrated NCC expression by crossing dnNRSF-Tg mice with mice lacking *CACNA1B*, encoding the α1B subunit of NCC. Because the *CACNA1B*$^{-/-}$ genotype has a high incidence of early mortality from an as yet unknown cause, we compared the phenotypes of dnNRSF-Tg;*CACNA1B*$^{+/+}$ mice with those of dnNRSF-Tg;*CACNA1B*$^{+/-}$ mice, in which NCC expression is reduced to ~52.9% of that in dnNRSF-Tg;*CACNA1B*$^{+/+}$ mice (*Figure 4A*). The gross appearance of *CACNA1B*$^{+/-}$ mice is normal, and they show no early mortality. Systolic blood pressures in dnNRSF-Tg;*CACNA1B*$^{+/-}$ and dnNRSF-Tg;*CACNA1B*$^{+/+}$ mice did not significantly differ, but they were mildly lower than in control WT (*CACNA1B*$^{+/+}$) mice (WT, 101.25 ± 7.26; *CACNA1B*$^{+/-}$, 91.25 ± 2.78; dnNRSF-Tg, 92 ± 4.38; dnNRSF-Tg;*CACNA1B*$^{+/-}$, 89.25 ± 2.14 mmHg) (*Figure 4B*). Similarly, heart rates did not differ between dnNRSF-Tg;*CACNA1B*$^{+/+}$ and dnNRSF-Tg;*CACNA1B*$^{+/-}$ mice, although they were slower in dnNRSF-Tg;*CACNA1B*$^{+/+}$ than in control WT mice, as reported previously (WT, 632.25 ± 26.36; *CACNA1B*$^{+/-}$, 594 ± 33.39; dnNRSF-Tg, 515.25 ± 14.71; dnNRSF-Tg;*CACNA1B*$^{+/-}$, 521.5 ± 23.32/min) (*Figure 4C*).[8] Body weights were comparable between the two dnNRSF-Tg groups (WT, 31.08 ± 1.11; *CACNA1B*$^{+/-}$, 29.53 ± 1.37; dnNRSF-Tg; 28.86 ± 1.19; dnNRSF-Tg;*CACNA1B*$^{+/-}$, 27.41 ± 1.09 g) (*Figure 4D*), but heart-to-body weight ratios were higher in dnNRSF-Tg;*CACNA1B*$^{+/+}$ than in WT (*CACNA1B*$^{+/+}$) mice and were significantly lower in dnNRSF-Tg;*CACNA1B*$^{+/-}$ than in dnNRSF-Tg;*CACNA1B*$^{+/+}$ mice (WT, 4.44 ± 0.04; *CACNA1B*$^{+/-}$, 4.51 ± 0.14; dnNRSF-Tg; 5.68 ± 0.21; dnNRSF-Tg;*CACNA1B*$^{+/-}$, 4.86 ± 0.18 mg/g) (*Figure 4E*). Lung-to-body weight ratios were comparable between the two dnNRSF-Tg groups (WT, 5.06 ± 0.22; *CACNA1B*$^{+/-}$, 4.68 ± 0.96; dnNRSF-Tg; 5.41 ± 0.09; dnNRSF-Tg; *CACNA1B*$^{+/-}$, 5.52 ± 0.26 mg/g) (*Figure 4F*). Echocardiographic analysis showed that left ventricular diastolic dimension (LVDd) was higher in dnNRSF-Tg;*CACNA1B*$^{+/+}$ than in WT mice, whereas EF was lower in dnNRSF-Tg;*CACNA1B*$^{+/+}$ than in WT mice, as was reported previously (*Figure 5A* and *B*).[8] In addition, LVDd was lower and EF was higher in dnNRSF-Tg;*CACNA1B*$^{+/-}$ than in dnNRSF-Tg;*CACNA1B*$^{+/+}$ mice (*Figure 5A* and *B* and *Table 1*).

Histological analysis revealed no significant difference between dnNRSF-Tg;*CACNA1B*$^{+/+}$ and dnNRSF-Tg;*CACNA1B*$^{+/-}$ mice, although %fibrotic area showed a trend towards being smaller in dnNRSF-Tg;*CACNA1B*$^{+/-}$ than in dnNRSF-Tg;*CACNA1B*$^{+/+}$ mice (*Figure 5C* and *D*). Expression of the fibrosis-related genes *Col1a1*, *Col3a1*, and *FN1* did not significantly differ between dnNRSF-Tg;*CACNA1B*$^{+/+}$ and dnNRSF-Tg;*CACNA1B*$^{+/-}$ mice (see Supplementary material online, *Figure S3A–C*), though there was a significant difference in the expression of *ANP* and *SERCA2* between these two genotypes (*Figure 5E* and *F*). Genetic reduction in *CACNA1B* also significantly affected expression of *CACNA1H* and *HCN2*, but not *HCN4*, in dnNRSF-Tg ventricles (see Supplementary material online, *Figure S3D–F*). All of these data demonstrate that genetic reduction of *CACNA1B* tends to ameliorate impaired cardiac function and pathological remodelling in dnNRSF-Tg mice. Furthermore, survival among dnNRSF-Tg;*CACNA1B*$^{+/-}$ mice was dramatically and significantly better than among control dnNRSF-Tg;*CACNA1B*$^{+/+}$ mice (*Figure 6A*), demonstrating that reduction of NCC prevents sudden arrhythmic death in dnNRSF-Tg mice.

3.5 Reducing *CACNA1B* expression improves autonomic function and decreases the occurrence of arrhythmias in dnNRSF-Tg mice

We also assessed autonomic nervous system activity in dnNRSF-Tg;*CACNA1B*$^{+/-}$ and dnNRSF-Tg;*CACNA1B*$^{+/+}$ mice. In HRV analyses, the reductions in LF and HF power otherwise seen in dnNRSF-Tg;*CACNA1B*$^{+/+}$ mice (LF, 1.288 ± 0.16; HF, 1.168 ± 0.108 m/s^2) were significantly ameliorated in dnNRSF-Tg;*CACNA1B*$^{+/-}$ mice (LF, 3.54 ± 0.47; HF, 3.075 ± 0.468 m/s^2), indicating a restoration of parasympathetic activity through reduction of NCC function (*Figure 6B* and *C*). In addition, we found that the increase in urinary excretion of norepinephrine seen in dnNRSF-Tg;*CACNA1B*$^{+/+}$ mice (0.428 ± 0.07 μg/day) was significantly ameliorated in dnNRSF-Tg;*CACNA1B*$^{+/-}$ mice (0.154 ± 0.05 μg/day) (*Figure 6D*). Finally, evaluation of arrhythmicity revealed that the incidences of both PVCs and VT were significantly lower in dnNRSF-Tg;*CACNA1B*$^{+/-}$ than in dnNRSF-Tg;*CACNA1B*$^{+/+}$ mice (PVC: WT, 0 ± 0; *CACNA1B*$^{+/-}$, 0 ± 0; dnNRSF-Tg, 239.08 ± 27.93; dnNRSF-Tg;*CACNA1B*$^{+/-}$, 3.21 ± 3.21 and VT: WT, 0 ± 0; *CACNA1B*$^{+/-}$, 0 ± 0; dnNRSF-Tg, 41.3 ± 12.69; dnNRSF-Tg;*CACNA1B*$^{+/-}$, 0.36 ± 0.36/h) (*Figure 6E* and *F*). These results demonstrate that genetic titration of *CACNA1B*, encoding NCC, corrected an imbalance between sympathetic and parasympathetic nervous system activities, which, at least in part, contributes to reducing malignant arrhythmias in dnNRSF-Tg mice in a manner similar to pharmacological NCC blockade.

4. Discussion

Autonomic dysregulation leading to increased sympathetic nerve activity and reduced parasympathetic nerve activity is reportedly associated with the increased arrhythmicity seen in patients with chronic heart failure.[2,22,23] NCCs play a major role in the release of norepinephrine at sympathetic nerve terminals.[7,24] Consequently, mice lacking *CACNA1B*, the gene encoding the α1 subunit of NCCs, exhibit a significantly impaired positive inotropic response.[7] In the present study, we found that pharmacological blockade of NCCs or their genetic titration improved the balance between sympathetic and parasympathetic nerve activities and prevented the sudden death and arrhythmicity otherwise seen in dnNRSF-Tg mice, a mouse model of sudden arrhythmic death associated with cardiac dysfunction.[8] The mode of death in these model mice is sudden and without overt oedema, pleural effusion, or apparent lung congestion, and all the telemetry data obtained at the time of death indicate VT/VF to be the cause.[8] Moreover, in an earlier study, we found that systemic administration of isoproterenol induced VT more frequently in dnNRSF-Tg than in WT mice.[11] Conversely, administration of a β-blocker led to a significant reduction in the incidence of sudden death among dnNRSF-Tg mice under conditions in which cardiac systolic function and remodelling were not affected (*Figure 3H–N*). These findings suggest that NCC blockade or genetic titration of NCC reduces the likelihood of sudden arrhythmic death, thereby improving survival.

Pharmacological interventions that reduce cardiac sympathetic activity have been shown to protect against arrhythmias,[25] while

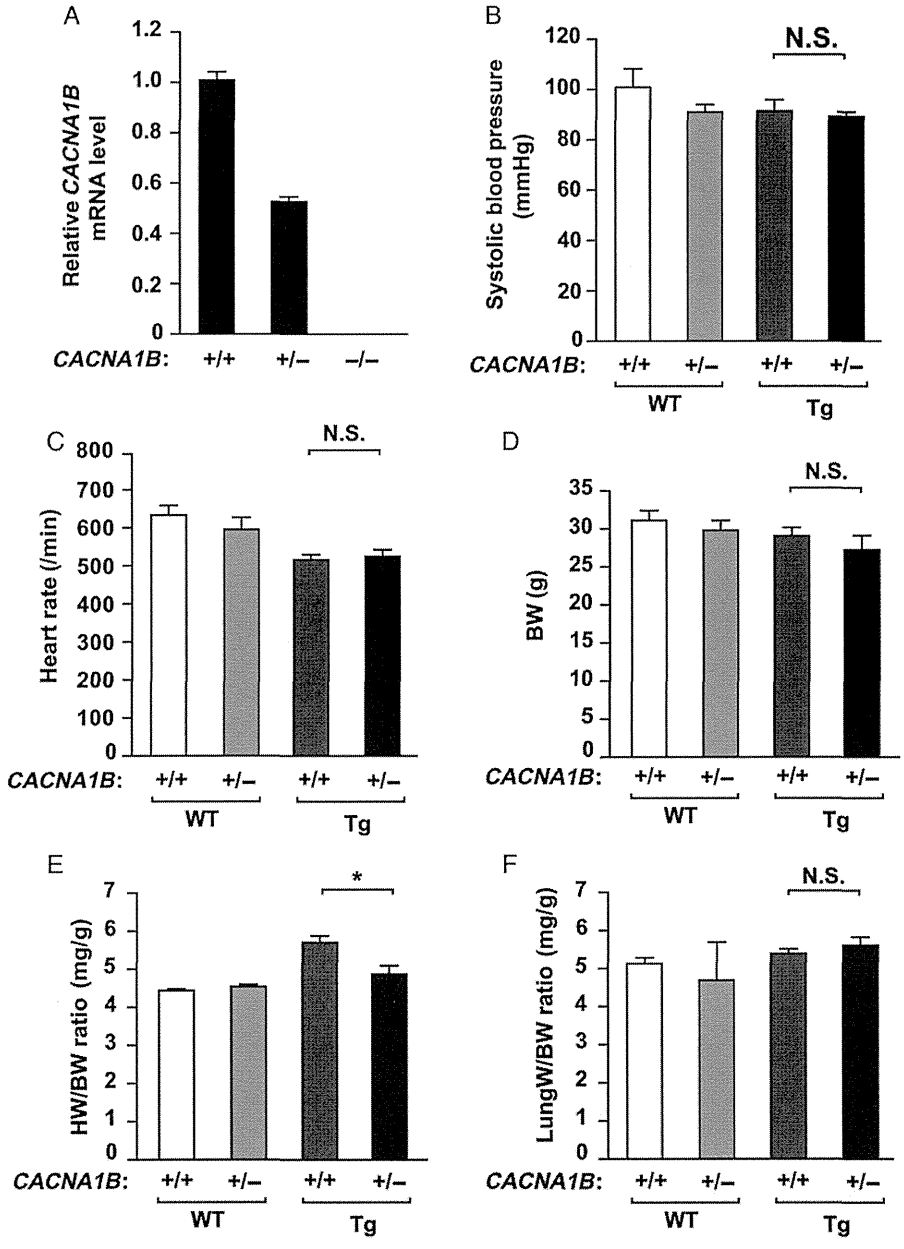

Figure 4 Effects of genetic titration of *CACNA1B* on hemodynamics and heart size in WT and dnNRSF-Tg mice. (*A*) CACNA1B mRNA expression in brains from 8-week-old CACNA1B$^{+/+}$, CACNA1B$^{+/-}$, and CACNA1B$^{-/-}$ mice; the level in CACNA1B$^{+/+}$ brain was assigned a value of 1.0. (*B* and *C*) Systolic blood pressures (*B*) and heart rates (*C*) in 20-week-old CACNA1B$^{+/+}$, CACNA1B$^{+/-}$, dnNRSF-Tg;CACNA1B$^{+/+}$, and dnNRSF-Tg;CACNA1B$^{+/-}$ mice. N.S.: not significant ($n = 4$ each). (*D*, *E*, and *F*) body weights (BW)(*D*), heart-to-body weight ratios (HW/BW) (*E*), and lung-to-body weight ratios (LungW/BW) (*F*) in 20-week-old CACNA1B$^{+/+}$, CACNA1B$^{+/-}$, dnNRSF-Tg;CACNA1B$^{+/+}$, and dnNRSF-Tg;CACNA1B$^{+/-}$ mice. *$P < 0.05$. N.S.: not significant. (BW and HW/BW: $n = 4$ for CACNA1B$^{+/+}$, $n = 6$ for CACNA1B$^{+/-}$, $n = 5$ for dnNRSF-Tg;CACNA1B$^{+/+}$, and $n = 7$ for dnNRSF-Tg;CACNA1B$^{+/-}$; LungW/BW: $n = 4$ for CACNA1B$^{+/+}$, $n = 6$ for CACNA1B$^{+/-}$ and dnNRSF-Tg;CACNA1B$^{+/-}$, and $n = 5$ for dnNRSF-Tg;CACNA1B$^{+/+}$). ANOVA with post hoc Fisher's tests was used for analysis. All data are shown as means ± SEM.

interventions that stimulate cardiac sympathetic activity provoke malignant arrhythmias.[2,26] In patients with heart failure, β-adrenoreceptor blockade reduces the incidence of sudden death;[27,28] however, β-blockers are not completely protective, and mortality remains high among patients with cardiac dysfunction, despite optimal β-blocker therapy.[27,28] It is therefore necessary to find other approaches to modulate sympathetic or parasympathetic activity. In that context, a clinical trial testing the effect of central modulation of sympathetic activity using moxonidine SR in patients with heart failure was terminated early due to an increase in mortality and morbidity in patients receiving the drug.[29] Thus, strong central inhibition of the sympathetic nervous system through imidazoline receptor stimulation appears not to

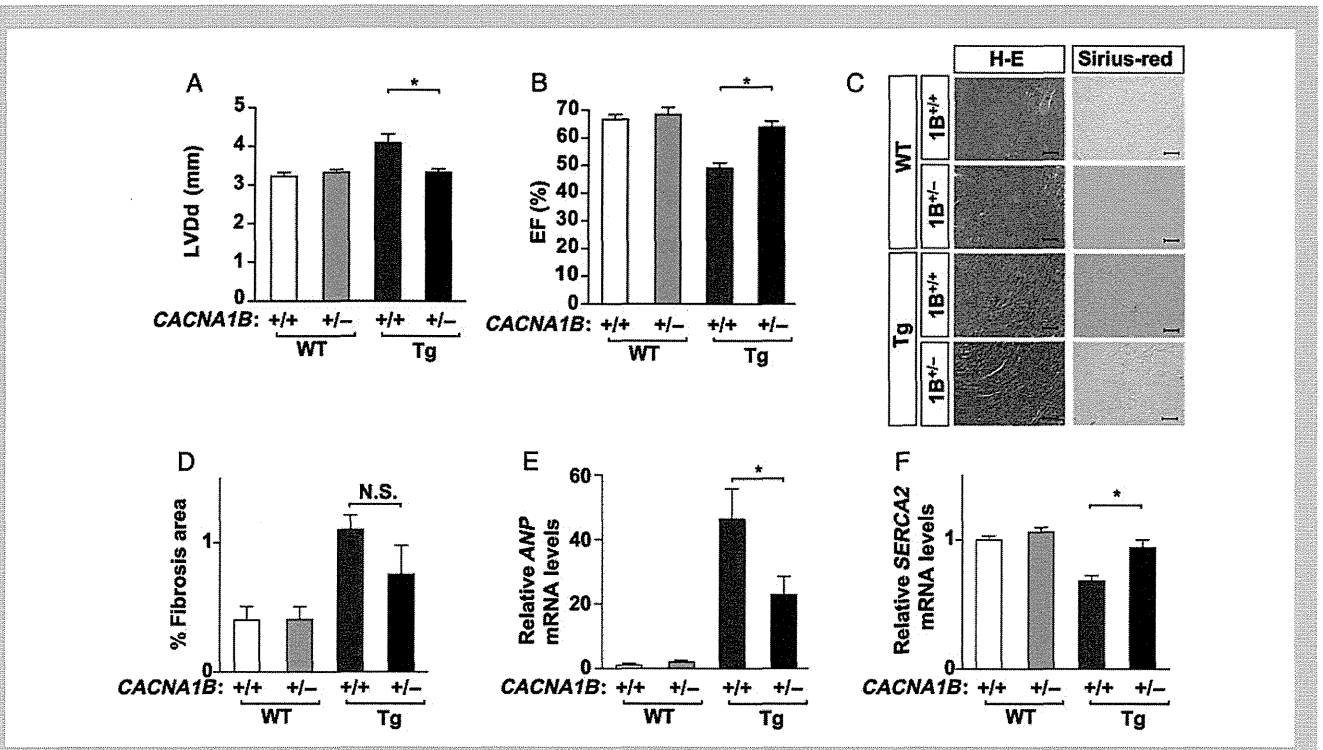

Figure 5 Effect of genetic titration of *CACNA1B* on cardiac structure and function in dnNRSF-Tg mice. (*A* and *B*) LVDd and EF assessed echocardiographically in 20-week-old CACNA1B$^{+/+}$, CACNA1B$^{+/-}$, CACNA1B$^{+/+}$; dnNRSF-Tg and CACNA1B$^{+/-}$; dnNRSF-Tg mice. *$P < 0.05$. ($n = 13$ for CACNA1B$^{+/+}$, $n = 14$ for CACNA1B$^{+/-}$, $n = 11$ for dnNRSF-Tg;CACNA1B$^{+/+}$, and $n = 15$ for dnNRSF-Tg;CACNA1B$^{+/-}$). (*C*) Histology of hearts from 20-week-old CACNA1B$^{+/+}$, CACNA1B$^{+/-}$, dnNRSF-Tg;CACNA1B$^{+/+}$ and dnNRSF-Tg;CACNA1B$^{+/-}$ mice. H-E, haematoxylin-eosin staining; Sirius-red, Sirius-red staining. Scale bars = 100 μm. (*D*) %Fibrotic area in the indicated groups ($n = 4$ for CACNA1B$^{+/+}$, $n = 6$ for CACNA1B$^{+/-}$, $n = 5$ for dnNRSF-Tg;CACNA1B$^{+/+}$, and $n = 7$ for dnNRSF-Tg;CACNA1B$^{+/-}$). N.S.: not significant. (*E* and *F*) Relative levels of ANP and SERCA2 mRNA in cardiac ventricles from 20-week-old CACNA1B$^{+/+}$, CACNA1B$^{+/-}$, dnNRSF-Tg;CACNA1B$^{+/+}$ and dnNRSF-Tg;CACNA1B$^{+/-}$ mice ($n = 4$ for CACNA1B$^{+/+}$, $n = 6$ for CACNA1B$^{+/-}$, and $n = 5$ for dnNRSF-Tg;CACNA1B$^{+/+}$ and dnNRSF-Tg;CACNA1B$^{+/-}$); levels in CACNA1B$^{+/+}$ ventricles were assigned a value of 1.0. *$P < 0.05$. ANOVA with post hoc Fisher's tests was used for analysis. All data are shown as means ± SEM.

protect against lethal arrhythmias. NCCs are localized at peripheral sympathetic nerve terminals, where they regulate the release of neurotransmitters (e.g. catecholamines), thereby modulating sympathetic activity.[4–6] Our findings suggest that, by correcting their autonomic dysregulation, NCC blockade could be an effective approach to preventing sudden arrhythmic death in patients with heart failure.

Cilnidipine failed to prevent the decline in cardiac function in dnNRSF-Tg mice, whereas genetic titration tended to ameliorate the adverse cardiac remodelling and cardiac dysfunction seen in dnNRSF-Tg mice (*Figures 2A–H*, *4E*, and *5A–F* and *Table 1*). The reasons for the difference in the effects on cardiac function between cilnidipine and genetic titration of NCCs remain unclear at present. It may be that cilnidipine's ability to block L-type Ca^{2+} channels has a detrimental effect on cardiac function, as L-type Ca^{2+} channel blockers can adversely affect the progression of heart failure.[30] Other possibilities are that the relatively low dose of cilnidipine used in this study was not sufficient to prevent the progression of cardiac dysfunction, though it did prevent lethal arrhythmias, or that the NCC inhibition achieved in *CACNA1B*$^{+/-}$ mice was more prolonged and more stable than that achieved with cilnidipine, which was not started until the mice were 8 weeks of age. The effects on NCCs expressed in the central nervous system could also differ between cilnidipine and genetic titration, as cilnidipine has little ability to cross the blood–brain barrier.[31] These differences suggest the underlying mechanisms involved in the reduced incidence of lethal arrhythmias, and the prolonged survival differ somewhat between cilnidipine treatment and genetic titration of *CACNA1B* in this study. Cilnidipine treatment, which improved autonomic imbalance and reduced lethal arrhythmias without affecting cardiac remodelling, mainly suppressed the triggering of lethal arrhythmias induced by autonomic imbalance. On the other hand, genetic titration of *CACNA1B*, which improved autonomic imbalance and also tended to prevent adverse cardiac remodelling, suppressed lethal arrhythmias and improved survival in two ways: it inhibited the triggering of arrhythmias and also suppressed the generation of arrhythmogenic substrates. In both cases, correcting the autonomic imbalance associates with a reduction in the incidence of sudden death attributable to lethal arrhythmias in dnNRSF-Tg. However, because it is not possible to completely exclude the possibility that some dnNRSF-Tg mice (especially older mice) die due to congestive heart failure, irrespective of arrhythmias, there is a possibility that genetic deletion of NCC may also prevent this mode of death in addition to sudden arrhythmic death in dnNRSF-Tg mice through suppression of excessive sympathetic activity.

In the present study, both pharmacological blockade of NCCs and their genetic titration not only repressed sympathetic activity, as demonstrated by a reduction in urinary norepinephrine levels, but also restored parasympathetic activity, as indicated by HRV analyses. The precise

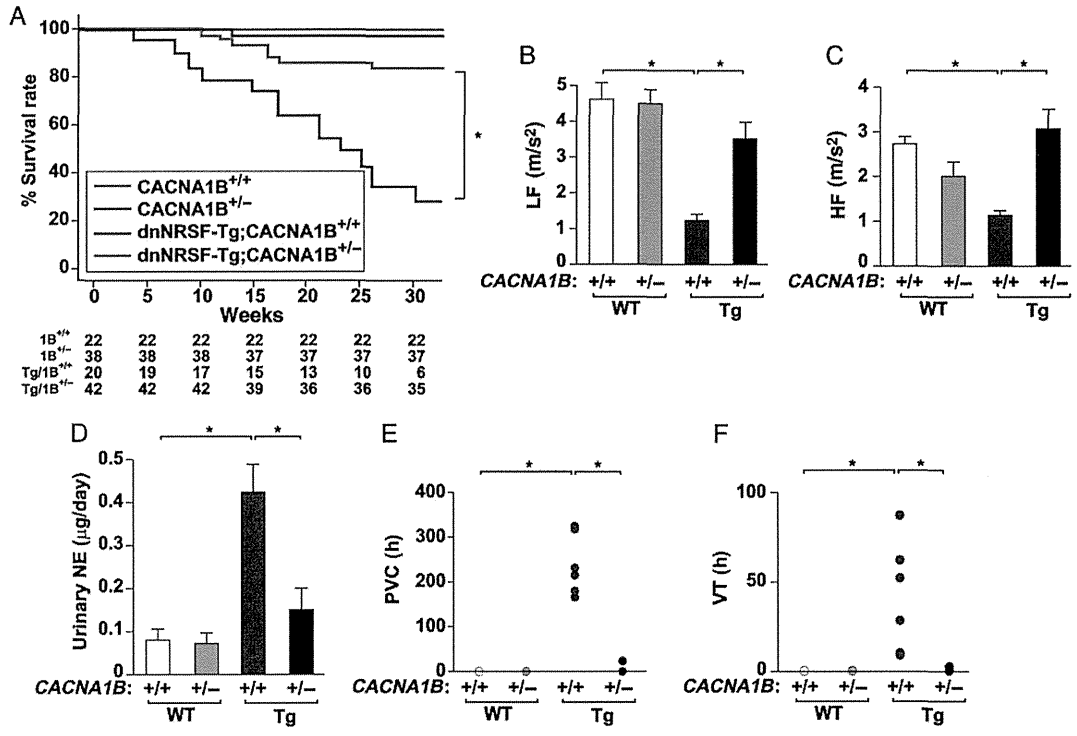

Figure 6 Genetic titration of *CACNA1B* restores cardiac autonomic nervous system balance and reduces arrhythmias in dnNRSF-Tg mice. (*A*) Kaplan–Meyer survival curves for CACNA1B$^{+/+}$ (1B$^{+/+}$), CACNA1B$^{+/-}$ (1B$^{+/-}$), dnNRSF-Tg;CACNA1B$^{+/+}$ (Tg/1B$^{+/+}$), and dnNRSF-Tg;CACNA1B$^{+/-}$ (Tg/1B$^{+/-}$) mice. Curves cover the span from birth to 32 weeks of age. Log-rank test was used for analysis. *$P < 0.05$ ($n = 22$ for CACNA1B$^{+/+}$, $n = 38$ for CACNA1B$^{+/-}$, $n = 20$ for dnNRSF-Tg;CACNA1B$^{+/+}$, and $n = 42$ for dnNRSF-Tg;CACNA1B$^{+/-}$). The numbers of mice alive in each group at the end of each period are shown at the bottom of the figure. (*B* and *C*) Average power of the LF (*B*) and HF (*C*) components of heart rate variability (HRV) recorded over a 24-h period in 20-week-old CACNA1B$^{+/+}$, CACNA1B$^{+/-}$, dnNRSF-Tg;CACNA1B$^{+/+}$, and dnNRSF-Tg;CACNA1B$^{+/-}$ mice. *$P < 0.05$ ($n = 5$ for CACNA1B$^{+/+}$, $n = 7$ for CACNA1B$^{+/-}$, $n = 6$ for dnNRSF-Tg;CACNA1B$^{+/+}$, and $n = 7$ for dnNRSF-Tg;CACNA1B$^{+/-}$). (*D*) Urinary norepinephrine (NE) levels in 20-week-old CACNA1B$^{+/+}$, CACNA1B$^{+/-}$, dnNRSF-Tg;CACNA1B$^{+/+}$, and dnNRSF-Tg;CACNA1B$^{+/-}$ mice. *$P < 0.05$ ($n = 5$ for CACNA1B$^{+/-}$, $n = 6$ for CACNA1B$^{+/+}$, dnNRSF-Tg;CACNA1B$^{+/+}$, and dnNRSF-Tg;CACNA1B$^{+/-}$). (*E* and *F*) Numbers of PVC (*E*) and VT (*F*) recorded using a telemetry system in 20-week-old CACNA1B$^{+/+}$, CACNA1B$^{+/-}$, dnNRSF-Tg;CACNA1B$^{+/+}$, and dnNRSF-Tg;CACNA1B$^{+/-}$ mice are shown by dot plot. *$P < 0.0083$ ($n = 5$ for CACNA1B$^{+/+}$, $n = 7$ for CACNA1B$^{+/-}$, $n = 6$ for dnNRSF-Tg;CACNA1B$^{+/+}$, and $n = 7$ for dnNRSF-Tg;CACNA1B$^{+/-}$). All data in *B*–*D* are shown as means ± SEM. ANOVA with post hoc Fisher's tests was used for analysis, except for numbers of arrhythmias (*E* and *F*). Numbers of arrhythmias were analyzed using Kruskal–Wallis non-parametric ANOVA followed by the Bonferroni correction.

mechanism by which NCC inhibition improves parasympathetic activity is not clear at present. However, accumulating data indicate the sympathetic and parasympathetic nervous systems interact via several mechanisms at both the central and peripheral levels of the neuraxis.[32] NCC inhibition-induced reductions in sympathetic activity may affect these interactions, ameliorating the reduction in parasympathetic activity, as was observed in dnNRSF-Tg mice. In humans, cilnidipine reportedly enhances parasympathetic activity in hypertensive patients while exerting a concomitant sympathoinhibitory effect.[12,13] Moreover, there is now much evidence showing the anti-arrhythmic effects of parasympathetic nervous activation. This suggests that, in addition to a reduction in sympathetic activity, an increase in parasympathetic activity likely contributes to the protective effects of NCC inhibition observed in this study.[27] Although further investigation is necessary, our study suggests that agents able to selectively block NCCs could be clinically useful for the prevention of sudden arrhythmic death in patients with heart failure.

Supplementary material

Supplementary material is available at *Cardiovascular Research* online.

Acknowledgements

We thank Ms Yukari Kubo for her excellent secretarial work and Ms Aoi Fujishima, Ms Akiko Abe, Mr Miku Ohya, and Ms Mizuho Takemura for their excellent technical support.

Conflict of interest: none declared.

Funding

This research was supported by Grants-in-Aid for Scientific Research from the Japan Society for the Promotion of Science (23390210, 24659386 to K.K., 24591095 to H.K., 22590810 to Y.N., 21229013 to N.K.); the Japanese Ministry of Health, Labor and Welfare (N.K.); the Japan Foundation for Applied Enzymology (K.K.); the UBE foundation (K.K.); the Ichiro Kanehara

Foundation (K.K.); the Takeda Science Foundation (K.K.); the Hoh-ansha Foundation (K.K.); the SENSHIN Medical Research Foundation (K.K.).

References

1. Tomaselli GF, Marban E. Electrophysiological remodeling in hypertrophy and heart failure. *Cardiovasc Res* 1999;**42**:270–283.
2. Anderson KP. Sympathetic nervous system activity and ventricular tachyarrhythmias: recent advances. *Ann Noninvasive Electrocardiol* 2003;**8**:75–89.
3. Chen PS, Chen LS, Cao JM, Sharifi B, Karagueuzian HS, Fishbein MC. Sympathetic nerve sprouting, electrical remodeling and the mechanisms of sudden cardiac death. *Cardiovasc Res* 2001;**50**:409–416.
4. Mori Y, Nishida M, Shimizu S, Ishii M, Yoshinaga T, Ino M, Sawada K, Niidome T. Ca(2+) channel alpha(1B) subunit (Ca(V) 2.2) knockout mouse reveals a predominant role of N-type channels in the sympathetic regulation of the circulatory system. *Trends Cardiovasc Med* 2002;**12**:270–275.
5. Hirning LD, Fox AP, McCleskey EW, Olivera BM, Thayer SA, Miller RJ, Tsien RW. Dominant role of N-type Ca2+ channels in evoked release of norepinephrine from sympathetic neurons. *Science* 1988;**239**:57–61.
6. Fujita Y, Mynlieff M, Dirksen RT, Kim MS, Niidome T, Nakai J, Friedrich T, Iwabe N, Miyata T, Furuichi T, Furutama D, Mikoshiba K, Mori Y, Beam KG. Primary structure and functional expression of the omega-conotoxin-sensitive N-type calcium channel from rabbit brain. *Neuron* 1993;**10**:585–598.
7. Ino M, Yoshinaga T, Wakamori M, Miyamoto N, Takahashi E, Sonoda J, Kagaya T, Oki T, Nagasu T, Nishizawa Y, Tanaka I, Imoto K, Aizawa S, Koch S, Schwartz A, Niidome T, Sawada K, Mori Y. Functional disorders of the sympathetic nervous system in mice lacking the alpha 1B subunit (Cav 2.2) of N-type calcium channels. *Proc Natl Acad Sci USA* 2001;**98**:5323–5328.
8. Kuwahara K, Saito Y, Takano M, Arai Y, Yasuno S, Nakagawa Y, Takahashi N, Adachi Y, Takemura G, Horie M, Miyamoto Y, Morisaki T, Kuratomi S, Noma A, Fujiwara H, Yoshimasa Y, Kinoshita H, Kawakami R, Kishimoto I, Nakanishi M, Usami S, Harada M, Nakao K. NRSF regulates the fetal cardiac gene program and maintains normal cardiac structure and function. *EMBO J* 2003;**22**:6310–6321.
9. Kuwabara Y, Kuwahara K, Takano M, Kinoshita H, Arai Y, Yasuno S, Nakagawa Y, Igata S, Usami S, Minami T, Yamada Y, Nakao K, Yamada C, Shibata J, Nishikimi T, Ueshima K, Nakao K. Increased expression of HCN channels in the ventricular myocardium contributes to enhanced arrhythmicity in mouse failing hearts. *J Am Heart Assoc* 2013;**2**: e000150.
10. Takano M, Kinoshita H, Shioya T, Itoh M, Nakao K, Kuwahara K. Pathophysiological remodeling of mouse cardiac myocytes expressing dominant negative mutant of neuron restrictive silencing factor. *Circ J* 2010;**74**:2712–2719.
11. Kinoshita H, Kuwahara K, Takano M, Arai Y, Kuwabara Y, Yasuno S, Nakagawa Y, Nakanishi M, Harada M, Fujiwara M, Murakami M, Ueshima K, Nakao K. T-type Ca2+ channel blockade prevents sudden death in mice with heart failure. *Circulation* 2009; **120**:743–752.
12. Kishi T, Hirooka Y, Konno S, Sunagawa K. Cilnidipine inhibits the sympathetic nerve activity and improves baroreflex sensitivity in patients with hypertension. *Clin Exp Hypertens* 2009;**31**:241–249.
13. Ogura C, Ono K, Miyamoto S, Ikai A, Mitani S, Sugimoto N, Tanaka S, Fujita M. L/T-type and L/N-type calcium-channel blockers attenuate cardiac sympathetic nerve activity in patients with hypertension. *Blood Press* 2012;**21**:367–371.
14. Egashira N, Okuno R, Abe M, Matsushita M, Mishima K, Iwasaki K, Oishi R, Nishimura R, Matsumoto Y, Fujiwara M. Calcium-channel antagonists inhibit marble-burying behavior in mice. *J Pharmacol Sci* 2008;**108**:140–143.
15. Lei B, Nakano D, Fujisawa Y, Liu Y, Hitomi H, Kobori H, Mori H, Masaki T, Asanuma K, Tomino Y, Nishiyama A. N-type calcium channel inhibition with cilnidipine elicits glomerular podocyte protection independent of sympathetic nerve inhibition. *J Pharmacol Sci* 2012;**119**:359–367.
16. Uneyama H, Uchida H, Konda T, Yoshimoto R, Akaike N. Selectivity of dihydropyridines for cardiac L-type and sympathetic N-type Ca2+ channels. *Eur J Pharmacol* 1999;**373**: 93–100.
17. Fujii S, Kameyama K, Hosono M, Hayashi Y, Kitamura K. Effect of cilnidipine, a novel dihydropyridine Ca++-channel antagonist, on N-type Ca++ channel in rat dorsal root ganglion neurons. *J Pharmacol Exp Ther* 1997;**280**:1184–1191.
18. Johnson R, Gamblin RJ, Ooi L, Bruce AW, Donaldson IJ, Westhead DR, Wood IC, Jackson RM, Buckley NJ. Identification of the REST regulon reveals extensive transposable element-mediated binding site duplication. *Nucleic Acids Res* 2006;**34**:3862–3877.
19. Heart rate variability. Standards of measurement, physiological interpretation, and clinical use. Task Force of the European Society of Cardiology and the North American Society of Pacing and Electrophysiology. *Eur Heart J* 1996;**17**:354–381.
20. La Rovere MT, Pinna GD, Maestri R, Mortara A, Capomolla S, Febo O, Ferrari R, Franchini M, Gnemmi M, Opasich C, Riccardi PG, Traversi E, Cobelli F. Short-term heart rate variability strongly predicts sudden cardiac death in chronic heart failure patients. *Circulation* 2003;**107**:565–570.
21. Just A, Faulhaber J, Ehmke H. Autonomic cardiovascular control in conscious mice. *Am J Physiol Regul Integr Comp Physiol* 2000;**279**:R2214–e002221.
22. Brack KE, Winter J, Ng GA. Mechanisms underlying the autonomic modulation of ventricular fibrillation initiation-tentative prophylactic properties of vagus nerve stimulation on malignant arrhythmias in heart failure. *Heart Fail Rev* 2013;**18**:389–408.
23. Schwartz PJ, La Rovere MT, Vanoli E. Autonomic nervous system and sudden cardiac death. Experimental basis and clinical observations for post-myocardial infarction risk stratification. *Circulation* 1992;**85**:I77–I91.
24. Molderings GJ, Likungu J, Gothert M. N-Type calcium channels control sympathetic neurotransmission in human heart atrium. *Circulation* 2000;**101**:403–407.
25. Billman GE. Cardiac autonomic neural remodeling and susceptibility to sudden cardiac death: effect of endurance exercise training. *Am J Physiol Heart Circ Physiol* 2009;**297**: H1171–H1193.
26. Volders PG. Novel insights into the role of the sympathetic nervous system in cardiac arrhythmogenesis. *Heart Rhythm* 2010;**7**:1900–1906.
27. Packer M, Coats AJ, Fowler MB, Katus HA, Krum H, Mohacsi P, Rouleau JL, Tendera M, Castaigne A, Roecker EB, Schultz MK, DeMets DL. Effect of carvedilol on survival in severe chronic heart failure. *N Engl J Med* 2001;**344**:1651–1658.
28. The Cardiac Insufficiency Bisoprolol Study II (CIBIS-II): a randomised trial. *Lancet* 1999; **353**:9–13.
29. Cohn JN, Pfeffer MA, Rouleau J, Sharpe N, Swedberg K, Straub M, Wiltse C, Wright TJ. Adverse mortality effect of central sympathetic inhibition with sustained-release moxonidine in patients with heart failure (MOXCON). *Eur J Heart Fail* 2003;**5**:659–667.
30. Mahe I, Chassany O, Grenard AS, Caulin C, Bergmann JF. Defining the role of calcium channel antagonists in heart failure due to systolic dysfunction. *Am J Cardiovasc Drugs* 2003;**3**:33–41.
31. Watanabe K, Dozen M, Hayashi Y. Effect of cilnidipine (FRC-8653) on autoregulation of cerebral blood flow. *Nihon Yakurigaku Zasshi* 1995;**106**:393–399.
32. Ondicova K, Mravec B. Multilevel interactions between the sympathetic and parasympathetic nervous systems: a minireview. *Endocr Regul* 2010;**44**:69–75.

OPEN ACCESS Freely available online

PLOS | ONE

The Effects of Super-Flux (High Performance) Dialyzer on Plasma Glycosylated Pro-B-Type Natriuretic Peptide (proBNP) and Glycosylated N-Terminal proBNP in End-Stage Renal Disease Patients on Dialysis

Yasuaki Nakagawa[1], Toshio Nishikimi[1]*, Koichiro Kuwahara[1], Shinji Yasuno[2], Hideyuki Kinoshita[1], Yoshihiro Kuwabara[1], Kazuhiro Nakao[1], Takeya Minami[1], Chinatsu Yamada[1], Kenji Ueshima[2], Yoshihiro Ikeda[3], Hiroyuki Okamoto[4], Kazukiyo Horii[4], Kiyoshi Nagata[4], Kenji Kangawa[5], Naoto Minamino[6], Kazuwa Nakao[1]

1 Department of Medicine and Clinical Science, Kyoto University Graduate School of Medicine, Kyoto, Japan, **2** Department of EBM Research, Kyoto University Hospital, Institute for Advancement of Clinical and Translational Science, Kyoto, Japan, **3** Medical corporation, Ikeda Clinic, Kyoto, Japan, **4** Diagnostics Division, Shionogi & Co., Ltd, Oska, Japan, **5** Department of Biochemistry, National Cerebral and Cardiovascular Center Research Institute, Fujishirodai, Suita, Osaka, Japan, **6** Department of Molecular Pharmacology, National Cerebral and Cardiovascular Center Research Institute, Fujishirodai, Suita, Osaka, Japan

Abstract

Background: Plasma BNP levels are predictive of prognosis in hemodialysis patients. However, recent studies showed that the current BNP immunoassay cross-reacts with glycosylated proBNP, and the NT-proBNP assay underestimates glycosylated NT-proBNP. In addition, the recently developed high performance dialyzer removes medium-sized molecular solutes such as β2-microgloburin. We therefore investigated the effects of high performance dialysis on measured levels of glycosylated proBNP, glycosylated NT-proBNP and other BNP-related peptides in end-stage renal disease (ESRD) patients on hemodialysis.

Method: The relationships between clinical parameters and BNP-related molecule were also investigated. We used our newly developed immunoassay to measure plasma total BNP and proBNP in 105 normal subjects and 36 ESRD patients before and after hemodialysis. Plasma NT-proBNP was measured using Elecsys II after treatment with or without deglycosylating enzymes. We also measured plasma ANP and cGMP using radioimmunoassays.

Results: All the measured BNP-related peptides were significantly higher in ESRD patients than healthy subjects. Total BNP (−38.9%), proBNP (−29.7%), glycoNT-proBNP (−45.5%), nonglycoNT-proBNP (−53.4%), ANP (−50.4%) and cGMP (−72.1%) were all significantly reduced after hemodialysis, and the magnitude of the reduction appeared molecular weight-dependent. Both the proBNP/total BNP and glycoNT-proBNP/nonglycoNT-proBNP ratios were increased after hemodialysis. The former correlated positively with hemodialysis vintage and negatively with systolic blood pressure, while the latter correlated positively with parathyroid hormone levels.

Conclusion: These results suggest that hemodialysis using super-flux dialyzer removes BNP-related peptides in a nearly molecular weight-dependent manner. The ProBNP/total BNP and glycoNT-proBNP/nonglycoNT-proBNP ratios appear to be influenced by hemodialysis-related parameters in ESRD patients on hemodialysis.

Citation: Nakagawa Y, Nishikimi T, Kuwahara K, Yasuno S, Kinoshita H, et al. (2014) The Effects of Super-Flux (High Performance) Dialyzer on Plasma Glycosylated Pro-B-Type Natriuretic Peptide (proBNP) and Glycosylated N-Terminal proBNP in End-Stage Renal Disease Patients on Dialysis. PLoS ONE 9(3): e92314. doi:10.1371/journal.pone.0092314

Editor: Emmanuel A. Burdmann, University of Sao Paulo Medical School, Brazil

Received October 31, 2013; **Accepted** February 20, 2014; **Published** March 25, 2014

Funding: This study was supported in part by Scientific Research Grants-in-Aid 20590837 and 23591041 from the Ministry of Education, Culture, Sports, Science and Technology of Japan (to T. Nishikimi); a grant (AS 232Z01302F) from the Japan Science and Technology Agency (to T. Nishikimi); and a grant from the Suzuken Memorial Foundation (to T. Nishikimi). The funders had no role in study design, data collection and analysis, decision to publish, or preparation of the manuscript.

Competing Interests: HO, KH, and KN are employees of Shionogi & Co., Ltd. Shionogi Company previously developed the BNP kit used in this study (Patent name: monoclonal antibody recognizing for C-terminal region of BNP and Patent number: 665850) and intend to develop a new assay kit for proBNP. There are no further patents, products in development or marketed products to declare. This does not alter the authors' adherence to all the PLOS ONE policies on sharing data and materials.

* E-mail: nishikim@kuhp.kyoto-u.ac.jp

Introduction

Hemodialysis patients exhibit a greatly heightened risk of cardiovascular morbidity and mortality. For example, these patients experience an extremely high prevalence of left ventricular hypertrophy and heart failure. Consequently, there is a great need for a good clinical biomarker enabling early identification of dialysis patients at risk of cardiovascular events and mortality, as well as earlier aggressive intervention.

B-type natriuretic peptide (BNP; also termed brain natriuretic peptide) is a cardiac hormone produced and secreted mainly by the ventricles; another cardiac hormone, atrial natriuretic peptide (ANP), is produced and secreted by the atria. [1] Ventricular wall stress and/or ischemia stimulate expression of the BNP precursor proBNP [2,3], which is thought to be cleaved to BNP-32 (BNP or mature BNP) and N-terminal proBNP (NT-proBNP) prior to its secretion [4]. Plasma levels of BNP, NT-proBNP and ANP are elevated in patients with cardiac hypertrophy or heart failure. [5] They are also elevated in patients with chronic kidney disease, especially those receiving dialysis. [6] This is likely related to left ventricular dysfunction as well as to reduced clearance and increased plasma volume. It is widely recognized that cardiac function is a major confounder influencing levels of these peptides in dialysis patients. Thus, even in dialysis patients with end-stage renal disease (ESRD), BNP is used for diagnosis and evaluation of the severity of heart failure and is predictive of patient prognosis. [7].

Recent studies have shown that unprocessed precursor proBNP circulates in healthy individuals [8], and that its levels in plasma are increased in patients with severe heart failure. This is noteworthy in part because the immunoassay system currently being used to measure BNP also detects proBNP (the anti-BNP antibody cross-reacts with proBNP). In fact, it appears that about 70% of the plasma BNP measured using the BNP immunoassay system is proBNP in healthy human subjects. [9] In addition, it was recently shown that recombinant proBNP derived from mammalian cells has seven sites capable of *O*-linked oligosaccharide attachment within the N-terminal portion of the peptide, [10] and that both proBNP and NT-proBNP are glycosylated in human plasma. [11] [12].

The latest dialyzer membranes used for hemodialysis have the ability to remove large solutes, like β2-microglobulin. The function of these "super-flux" membranes is to remove larger and protein-bound uremic toxins. Earlier reports showed that plasma BNP and ANP levels are reduced after hemodialysis using a "low-flux" membrane, most likely due to body fluid volume removal and/or dialyzer membrane-mediated removal. However, the effect of super-flux membranes on BNP and BNP-related molecules, such as glycosylated proBNP and glycosylated NT-proBNP, remains unknown. In the present study, therefore, we examined the levels of total BNP, proBNP, mature BNP, glycosylated NT-proBNP, nonglycosylated NT-proBNP, ANP and cGMP in ESRD patients, before and after hemodialysis using a super-flux membrane.

Subjects and Methods

Patients

105 healthy subjects and 36 ESRD patients attending routine outpatient hemodialysis sessions were included in the study. Ethical approval was granted by the Kyoto University Hospital Ethical Committee. The aims of study were explained to each participant, and written consent was obtained. All clinical investigations were conducted according to the principles expressed in the Declaration of Helsinki.

In the ESRD group, all the patients underwent regular hemodialysis three times a week. The clinical characteristics of the healthy subjects and ESRD patients in this study are listed in Table 1. In the ESRD group, all the patients were dialyzed using super-flux polysulphonedialyzers: PES-19SEa eco in 4 cases, PES-21SEa eco in 8 cases, PES25SEa eco in 3 cases (Nipro, Tokyo, Japan), PS-15EL in 4 cases, APS18EL in 4 cases, APS-21EL in 11 cases and KF-20C in 2 cases (Asahikasei, Tokyo Japan). The mean dialysis session time was 3.96±0.30 h, and the QB was 209±25.1 ml/h. Cardiac function, heart size and blood pressure were relatively well controlled. Total body fluid volume was estimated using the equation: body weight×0.6 [13]. The percent changes in total body fluid volume were calculated as: body weight change/calculated total body weight before hemodialysis.

Blood Sampling

Venous blood was collected before and immediately after dialysis for measurement of total BNP, proBNP, mature BNP, nonglycoNT-proBNP, glycoNT-proBNP, ANP and cGMP. Blood samples were transferred to chilled glass tubes containing disodium EDTA (1 mg/ml) and aprotinin (500 U/ml) and immediately centrifuged at 4°C, after which the resultant plasma was frozen and stored at −80°C until used. We also measured levels of hemoglobin, serum c-reactive protein, albumin and parathyroid hormone, among others.

Biochemical Analyses

Measurement of plasma ANP, cGMP, total BNP, proBNP, and mature BNP. Plasma ANP levels were measured using a specific immunoradiometric assay, while levels of cGMP were measured using a radioimmunoassay, as previously described.[10]

Plasma total BNP and proBNP levels were measured using an immunochemiluminescent assay, as previously described. [9] All BNP assays, regardless of the source (e.g., Shionogi, Biosite), cross-react with proBNP, because the two antibodies used in the assays recognize epitopes common to BNP and proBNP. For that reason, total BNP means the sum of proBNP plus mature BNP, most of which is BNP[1–32]. In the present study, we measured total BNP and proBNP separately and calculated the mature BNP as follows: mature BNP = total BNP − proBNP. [9].

Measurement of plasma glycoNT-proBNP and nonglycoNT-proBNP in HD patients. ProBNP is post-translationally glycosylated to varying degrees in its N-terminal region, at Thr36, Ser37, Ser44, Thr48, Ser53, Thr58 and Thr71. [10] NT-proBNP is similarly glycosylated. The Elecsys proBNP II system (Roche Diagnostics, Germany) is comprised of a capture monoclonal antibody that recognizes NT-proBNP[27–31] and a monoclonal signal antibody that recognizes NT-proBNP[42–46], which contains a glycosylation site at amino acid residue 44. [14] Notably, *O*-linked oligosaccharide attachment inhibits the binding of the signal antibody to NT-proBNP. [15,16] We therefore postulated that NT-proBNP measured using Elecsys proBNP II is actually only nonglycoNT-proBNP. To measure total NT-proBNP, plasma samples were incubated for 24 h at 37°C with or without a cocktail of deglycosylating enzymes, included *O*-glycosidase (Roche Diagnostics) and neuraminidase (Roche Diagnostics) at final concentrations of 4.25 and 42.5 mU/ml, respectively, as described previously. [10] [14] NT-proBNP levels were then measured using Elecsys proBNP II, after which the glycoNT-proBNP level was calculated as: total NT-proBNP – nonglycoNT-proBNP.

Echocardiographic measurements. An experienced echocardiographer without knowledge of the clinical features of the patients performed the echocardiography using a cardiac ultra-

Table 1. Clinical profiles of the healthy subjects and ESRD patients enrolled in this study.

	Healthy subjects (N = 105)	ESRD patients (N = 36)	p
Age, years	51.3±12.1	64.0±11.7	<0.0001
Sex, m/f	50/55	20/16	0.2663
BMI, kg/m^2	22.2±3.0	20.2±2.4	0.0005
HD vintage, year	(−)	11.2±8.9	
Before HD			
Systolic BP, mmHg	115.4±17.3	142.2±22.4	<0.0001
Diastolic BP, mmHg	73.9±13.0	71.4±10.8	0.3016
Mean BP, mmHg	87.7±14.0	95.0±13.1	0.0071
After HD			
Systolic BP, mmHg		128.5±19.9	
Diastolic BP, mmHg		69.9±9.4	
Mean BP, mmHg		89.5±11.2	
Inter-dialysis weight gain, kg		2.67±0.92	
CTR,%	44.4±4.6	49.7±5.0	<0.0001
BUN, mg/dl	14.0±3.1	59.3±17.2	<0.0001
Cre, mg/dl	0.76±0.14	10.59±1.27	<0.0001
Alb, g/dl	4.3±0.2	3.60±0.35	<0.0001
Hemoglobin, g/dl	14.0±1.3	10.62±1.15	<0.0001
Ht, %	43.1±3.6	32.1±3.6	<0.0001
Diabetes mellitus	(−)	27.8 (10)	
Anti-hypertensive drug	(−)		
Calcium channel blocker		44.4%(16)	
Alpha blocker		2.8%(1)	
Beta blocker		38.9%(14)	
ACEI		2.8%(1)	
ARB		36.1%(13)	
Nitrate		5.6.%(2)	
Digoxin		2.8%(1)	
Statin		25.0%(9)	
Aspirin		30.6%(11)	
Insulin		2.8%(1)	
Echocardiographic data	Not examined		
IVS thickness, mm		10.8±1.9	
PW thickness, mm		11.35±2.0	
LV mass index, g/m^2		131.7±37.0	
Left atrium diameter, mm		37.9±5.3	
LV end-diastolic diameter, mm		43.8±5.8	
LV end-systolic diameter, mm		26.6±6.1	
Ejection fraction, %		64.2±11.5	

doi:10.1371/journal.pone.0092314.t001

sound unit (Logic 500 MD; GE Healthcare, England) before hemodialysis in the ESRD group. Left atrial diameter, interventricular thickness, posterior wall thickness, left ventricular end-diastolic diameter and left ventricular end-systolic diameter were all measured. Fractional shortening (FS), left ventricular mass index (LVMI) and left ventricular ejection fraction (LVEF) were calculated using standard formulae according to the recommendations of the American Society of Echocardiography.

Gel filtration chromatography. We analyzed immunoreactive proBNP levels in plasma to determine whether it is glycosylated in hemodialysis patients. Eluate lyophilized after extraction on a Sep-Pak C18 column (Waters, Milford, MA, USA) was dissolved in phosphate buffer and incubated with or without a cocktail of deglycosylation enzymes for 24 h at 37°C, as described above. The eluate was then lyophilized again and dissolved in 30% acetonitrile containing 0.1% TFA. The resultant solution was separated by gel filtration high-performance liquid chromatography (HPLC) on a Superdex 75 10/300 GL column (10×300 mm×2, GE Healthcare) using the same buffer at a flow rate of 0.4 mL/min. The column effluent was fractionated every

minute into polypropylene tubes containing bovine serum albumin (100 mg), after which each fraction was analyzed using our recently developed total BNP and proBNP immunochemiluminescent assay [9].

Statistical Analyses

All values are expressed as means±SE. The statistical significance of differences between two groups was evaluated using Fisher's exact test or paired Student's t test, as appropriate. The distribution of plasma peptide levels was normalized by log transformation, when appropriate. The statistical significance of differences among three or more groups was evaluated using one-way analysis of variance followed by Bonferroni's multiple comparison test. Correlation coefficients were calculated using linear regression analysis. Values of $p<0.05$ were considered significant.

Results

The clinical profiles of the healthy subjects and ESRD patients enrolled in this study are shown in Table 1. The healthy subjects received no medication. Among the ESRD patients, 86% were prescribed antihypertensive medication (Table 1). The average percentage weight loss during hemodialysis was 4.9% (2.2% to 8.4%), with a post-dialysis relative extracellular fluid volume of 20.2% (11.1% to 31.5%). Standard two-dimensional transthoracic echocardiography revealed an average cardiac ejection fraction of 64% (36% to 92%), and the cardiothoracic ratio measured on posterior-anterior chest X-rays was 50±5%.

Plasma Concentrations of Total BNP, proBNP, Mature BNP, nonglycoNT-proBNP, glycoNT-proBNP, ANP and cGMP in Healthy Subjects and ESRD Patients Before Hemodialysis

Plasma levels of total BNP, proBNP, mature BNP, nonglycoNT-proBNP, glycoNT-proBNP, ANP and cGMP in healthy subjects and ESRD patients before hemodialysis are shown in Table 2. All seven parameters were significantly higher in the hemodialysis patients than the healthy subjects ($p<0.0001$). In addition, glycoNT-proBNP levels was significantly higher than nonglycoNT-proBNP in both groups. There was no significant difference in the glycoNT-proBNP/nonglycoNT-proBNP ratio (healthy subject vs. ESRD patients: 4.6±1.8 vs. 4.4±1.7; n.s.) between the two groups.

Differences in the Plasma Concentrations of Total BNP, proBNP, Mature BNP, nonglycoNT-proBNP, glycoNT-proBNP, ANP and cGMP before and after Hemodialysis

We next focused on the profile of natriuretic peptide-related molecules in ESRD patients. We initially evaluated the changes in plasma levels of total BNP, proBNP, mature BNP, nonglycoNT-proBNP, glycoNT-proBNP, ANP and cGMP associated with hemodialysis. As shown in Figure 1A, B, C, D, E, F and G, levels of all seven parameters were significantly lower after hemodialysis ($p<0.001$).

As shown in Figure 1H, the reduction ratios were calculated using the formula (A−B)/A, where A and B were the plasma concentrations before and after hemodialysis, and the values obtained give the relative magnitudes of the reductions. The reduction ratio for proBNP was smaller than the others, whereas the ratio for cGMP, which had the smallest molecular weight (MW = 523), was the largest among the molecules tested. The reduction ratio for mature BNP (MW = 3500) was significantly greater than that for proBNP, but was about the same as those for ANP (MW = 3000) and nonglycoNT-proBNP (MW = 8500). And not surprisingly, the reduction ratio for total BNP, which includes proBNP plus mature BNP, was between the ratios for mature BNP and proBNP.

It is well known that decreasing cardiac load reduces circulating levels of BNP and ANP, and that decreasing total body fluid volume could reduce cardiac preload. We therefore evaluated the relationship between dialysis-induced loss of body weight and total body fluid volume and the plasma levels of total BNP, proBNP, nonglycoNT-proBNP, glycoNT-proBNP and ANP. However, we found no significant correlation between the percent body weight change or percent total body fluid volume loss and the percent reduction of any of these peptides (Table 3).

Gel-filtration Chromatography Before and after Deglycosylation Procedure

Figure 2A shows two immunoreactive BNP peaks detected using the total BNP assay with gel filtration fractions. The first peak appeared in fractions 52–55 and the second peak in fractions 72–75. When subjected to gel filtration, recombinant proBNP, glycosylated proBNP and BNP were eluted mainly in fractions 53, 56 and 74, respectively. Treating the same plasma sample with an enzyme cocktail catalyzing deglycosylation shifted the first peak to fractions 54–56, which is consistent with the proBNP peak. These results suggest the major molecular form of proBNP in the plasma of hemodialysis patients is glycosylated proBNP.

Table 2. Natriuretic peptide-related molecules in healthy subjects and ESRD patients.

	Healthy subjects (n = 105)	ESRD patients (n = 36)	p
Total BNP, pM	1.8±22.0	35.7±34.4	<0.0001
proBNP, pM	1.2±1.2	22.6±22.7	<0.0001
Mature BNP, pM	0.6±0.8	13.1±12.9	<0.0001
Nonglyco-NT-proBNP, pM	44.8±64.5	600.3±779.1	<0.0001
Glyco-NT-proBNP, pM	173.0±157.3	1934.2±1829.5	<0.0001
ANP, pM	21.1±12.4	44.3±30.9	<0.0001
cGMP, nM	2.9±1.3	20.2±13.0	<0.0001

doi:10.1371/journal.pone.0092314.t002

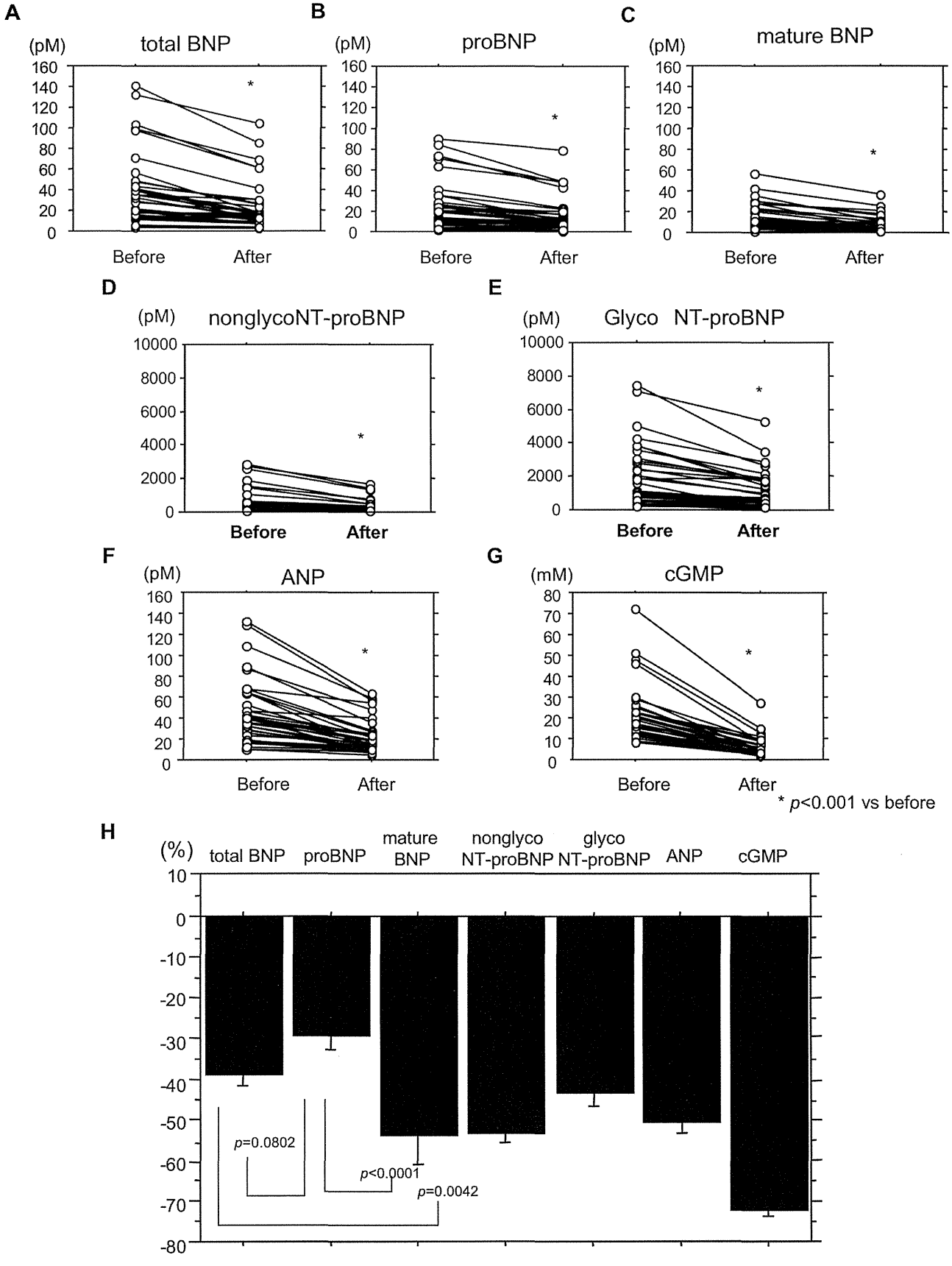

Figure 1. Changes in plasma levels of individual parameters during hemodialysis. (A–G) Individual changes in the levels of total BNP (A), proBNP (B), mature BNP (C), nonglycoNT-proBNP (D), glycoNT-proBNP (E), ANP (F) and cGMP (G) in ESRD patients during hemodialysis. Values are

means ± SE. *p<0.001 vs. before hemodialysis. Before, before hemodialysis; After, after hemodialysis. (H) Reduction ratios for total BNP, proBNP, mature BNP, nonglycoNT-proBNP, glycoNT-proBNP, ANP and cGMP in ESRD patients during hemodialysis. Values are means ± SE.
doi:10.1371/journal.pone.0092314.g001

Relationship between proBNP and Total BNP, Mature BNP, nonglycoNT-proBNP, glycoNT-proBNP and ANP

We next evaluated the relationships between proBNP and the other natriuretic peptide molecules in hemodialysis patients (Figure 2B, C, D, E and F). We found that levels of proBNP significantly correlated with those of total BNP, mature BNP, nonglycoNT-proBNP, glycoNT-proBNP and ANP, most of which are established biomarkers.

Relationship between cGMP and Total BNP, proBNP, Mature BNP, nonglycoNT-proBNP, glycoNT-proBNP and ANP in ESRD Patients before and after Hemodialysis

When we evaluated the correlation between the levels of cGMP and those of natriuretic peptide-related molecules, we found that levels of total BNP, proBNP, mature BNP, nonglycoNT-proBNP, glycoNT-proBNP and ANP all correlated significantly with cGMP, both before and after hemodialysis (Figure 3). In particular, proBNP appeared to correlate more strongly with cGMP before hemodialysis than did the other molecules. After hemodialysis, ANP showed the highest correlation with cGMP among the natriuretic peptide-related molecules.

ProBNP/Total BNP Ratios, Biochemical Parameters and Patient Profiles

It was previously suggested that the ratio of proBNP to total BNP varied widely, depending on the patient's heart failure status. [8] We next evaluated proBNP/total BNP ratios in ESRD patients. As shown in Figure 4, ProBNP/total BNP ratios were significantly increased after hemodialysis, which could, in part, reflect the fact that the relative reduction in proBNP was smaller than that for total BNP. There was also a significant (but weak) positive correlation with hemodialysis vintage. Upon examination of the patient profiles, we found no significant correlation between the proBNP/total BNP ratios and any other biochemical parameter. ProBNP/total BNP ratios showed weak but significant negative correlations with systolic and mean blood pressures ($R = -0.358$, $P = 0.014$, $R = -0.350$, $P = 0.036$), and tended toward a negative correlation with left atrial diameter ($R = -0.302$, $p = 0.073$).

NonglycoNT-proBNP and glycoNT-proBNP in Hemodialysis Patients

We also compared the levels of glycoNT-proBNP with those of nonglycoNT-proBNP in hemodialysis patients. We found that levels of glycoNT-proBNP were several times higher than those of nonglycoNT-proBNP in the patients before hemodialysis; nonetheless, the glycoNT-proBNP/nonglycoNT-proBNP ratio was significantly larger after hemodialysis than before it (Figure 5). This is in part because the relative reduction in nonglycoNT-proBNP during hemodialysis was significantly greater than that for glycoNT-proBNP. We then evaluated the correlations between the glycoNT-proBNP/nonglycoNT-proBNP ratios and other biochemical parameters, which revealed the ratio correlated significantly with serum parathyroid hormone levels in the patients, but not with serum calcium or phosphate levels (data not shown).

Discussion

Plasma BNP and NT-proBNP levels are elevated in patients with heart failure, [17] [18] [19] correlate strongly with LV filling pressure, and increase with increasing severity of heart failure evaluated based on New York Heart Association Class [20] [21], functional capacity [22], or systolic and diastolic dysfunction [23,24]. Even in patients with chronic kidney disease and ESRD, left ventricular end-diastolic wall stress remains a strong determinant of circulating BNP levels [25]. Moreover, in ESRD patients receiving long-term dialysis, BNP and NT-proBNP levels are strongly associated with the severity of LV hypertrophy and systolic dysfunction [6] [26,27,28,29,30], and their elevation also reflects the presence of myocardial ischemia and is indicative of the severity of coronary artery disease [31]. Finally, BNP and NT-proBNP are highly predictive of subsequent cardiac events and mortality in hemodialysis patients. [32].

It was once thought that proBNP is cleaved to BNP and NT-proBNP within cardiac myocytes and then secreted into the circulation. However, recent studies have shown that circulating levels of unprocessed precursor proBNP are elevated in heart failure. In addition, proBNP and NT-proBNP contain seven sites suitable for *O*-linked oligosaccharide attachment within their N-terminal regions. In the present study, therefore, we measured plasma levels of proBNP, total BNP, mature BNP, nonglycoNT-

Table 3. Correlation coefficients and p values relating changes in percent body weight or total body fluid volume to the percent reduction in natriuretic peptide-related molecules.

	% body weight change		% total body fluid volume change	
% Reduction rate	r	p	r	p
total BNP	−0.086	0.621	−0.096	0.580
mature BNP	−0.130	0.452	−0.124	0.474
proBNP	−0.039	0.823	−0.054	0.756
ANP	−0.117	0.500	0.119	0.493
nonglyco- NT-proBNP	−0.120	0.488	−0.122	0.483
glyco- NT-proBNP	−0.208	0.224	−0.209	0.222
cGMP	−0.047	0.785	−0.034	0.846

r is the correlation coefficient.
doi:10.1371/journal.pone.0092314.t003